



## Management of Rice tungro spread and control by sanitation measures for rice plants: Modeling and sensitivity analysis

Khurram Faiz<sup>1</sup>, Aqeel Ahmad<sup>1,\*</sup>, and Zafar Ullah<sup>2</sup>

<sup>1</sup>Department of Mathematics, Ghazi University D G Khan 32200, Pakistan.

<sup>2</sup>Division of Science and Technology, Department of Mathematics, University of Education, Lahore 54000, Pakistan.

### Abstract

Examining the model of rice tungro illness by observing how diseases spread within the community as a result of predators is the main goal of this study by developing new mathematical model. Following some measurements of infection rates for various plant stages, a mathematical model is developed utilizing the hypothesis developed for a healthy environment in order to investigate the various rates of rice tungro. In addition to studying the model's equilibrium and endemic points, the next generation method is used to determine the model's reproductive number at equilibrium points. Sensitivity analysis was developed to identify the most sensitive parameters and investigate the effects of variations in the rate of change under different circumstances. A suggested model is analyzed both qualitatively and quantitatively, with special attention paid to boundedness, positivity, and unique solutions. Both endemic and disease-free equilibrium points are examined for stability by globally validating the Lyapunov function. A two-step Lagrange polynomial method is applied in numerical simulations to investigate the effect of the fractional operator on the generalized form of the power law kernel for ongoing surveillance of the rice tungro virus and treatment strategies. The simulations show how different parameters affect the sickness. Simulations have been built to mimic the behavior and treatment of rice tungro disease caused by a splashing-rain attack and to put control measures in place for a healthy environment with a hypersensitive reaction (HR). Based on confirmed results for different plant species, this kind of research will be useful in determining how diseases spread and in creating management plans.

**Keywords.** Mathematical Modeling, Caputo, Sensitivity analysis, Rice tungro, Positiveness.

**2010 Mathematics Subject Classification.** 93A30, 49Q12, 52A21.

### 1. INTRODUCTION

The Sustainable Development Goals (SDGs) include promoting sustainable agriculture and ensuring food security. One strategy to guarantee food security is to make staple foods like rice a staple meal made from rice plants—available. Measures must be taken to prevent diseases like tungro disease from spreading among rice plants in order to achieve this goal. The primary vector responsible for spreading tungro disease among rice plants is the green leafhopper. If infection occurs during the nursery stage, plants will begin to show symptoms of tungro disease two to three weeks after planting. After rice is planted in the field, diseased and immature rice plants serve as the main source of inoculum. During a certain stage of growth, the number of infected plants can double. Immigrant insects were the source of the first infection peak, and infection with immigrant insect descendants was the reason for the second infection peak.

A key issue in global development is food security. Food security is defined as "the state in which all individuals, at all times, have physical and financial access to enough safe and nutritious food to meet their dietary needs and preferences for an active and healthy life" [19]. The issue of food security is significantly influenced by the agricultural sector. A sustainable approach to agricultural growth and food security involves raising agricultural production.

Received: 10 December 2024 ; Accepted: 26 October 2025.

\* Corresponding author. Email: aqeelahmad.740@gmail.com.

However, a number of issues, particularly with regard to food crop commodities, contribute to a decline in both the amount and quality of agricultural production. Plant susceptibility to disease, pests, weather, and climate change are some of the primary determinants of it [14]. A mathematical model for plant diseases was created to give a thorough explanation of how to characterize, evaluate, and forecast plant disease outbreaks in order to create and evaluate crop protection control measures and strategies [21]. Plant epidemiology presents a number of significant challenges for human and animal disease models. Nevertheless, modeling plant diseases is complicated by several distinctive features of plant epidemiology [12].

Rice (*Oryza sativa*) is the most significant food crop in developing countries, as it is a staple diet for over half of the world's population [18]. Since rice is a staple meal that many Asian communities depend on, rice harvests are currently the main source of concern. The prospective results of the rice varieties won't materialize if the plants are infected with the Tungro virus. There won't even be any repercussions if the Tungro virus infection occurs during the early vegetative stage. Tungro rice disease is caused by two different kinds of related Tungro viruses: the stem virus (Rice Tungro Bacilliform Virus: RTBV) and the spherical virus (Rice Tungro Spherical Virus: RTSV). Complicated symptoms will be displayed by rice plants infected with two varieties of the Tungro virus. The symptoms are less severe if the plant is just infected with RTBV, but they are completely absent if it is only infected with RTSV. The green leafhoppers *Nephotettix virescens* are the only semi-persistent carriers of both viruses. Rao discovered that as the vector population grew, so did the prevalence of RTV (Rice Tungro Virus) [23]. The tungro virus must be managed in order to stop the spread of illness. Taking into account integrated pest and disease control techniques, effective cultural practices, and varietal resistance [1]. The most common method for controlling the Tungro virus is through the use of insecticides. Spraying insecticides helps reduce the population of green leafhoppers, which in turn slows the spread of the virus. Several common pesticides can effectively manage green leafhopper populations.

Fractional calculus is in many scientific fields, including physics and engineering. Fractional order models are preferred over traditional integer order models because they can account for the genetic and memory components of systems [4]. Fractional-order derivatives can impact the spread of diseases, as seen in lung cancer and corona virus models [11]. The need for these models in reaction to social and economic unrest was highlighted by the COVID-19 epidemic [9]. In certain contexts, such as fuzzy environments, where fuzzy parameters are employed to account for the variation in parameter values among population members, certain disease models can be studied [13]. Using the ABC operator, they converted their mathematical model of immune system strengthening into a fractional-order model [22]. Building on the concept of immune system enhancement, they created a mathematical model that was transformed using the ABC operator into a fractional-order model. Their research aimed to evaluate the effectiveness of different treatment methods, with and without medication, for the early detection and treatment of the cholera virus [2]. Because of its early morbidity, mortality, shortened life expectancy, and financial consequences for patients, their employment, and the healthcare system, diabetes is a serious public health concern. One possible answer to this issue is a mathematical model that incorporates  $\beta$ -cells, insulin, glucose, and growth hormone [15]. Furthermore, a fractional order model for PCOS, one of the most common endocrine disorders among women of reproductive age, was developed using a unique technique that makes use of the memory effect of a fractional operator [3].

In several fields, ordinary differential equations (ODEs) are generalized to a non-integer order. For example, fractional differential operators (FDOs) are used to simulate physical models of many processes in pure and practical research. Since they are nonlocal operators, the computation of a time-fractional derivative at a given moment requires knowledge of all past periods. Atangana-Toufik method [5], Caputo and Caputo Fabrizio fractional derivative operator [8], caputo fabrizio derivative [16], Atangana-Baleanu-Caputo and Liouville-Caputo fractional derivatives [17], Fractional difference operator [7], and Modified fractional difference operator [6] are a few examples of sophisticated fractional differential operators used in mathematical modeling for models like these. While Leibniz and L'Hospital first discussed the ideas of non integer integral and derivative in 1695, Liouville and Riemann provided the first formulation of fractional derivative towards the last of the nineteenth century [24]. Over the past thirty years, research on fractional calculus has assisted in the resolution of practical issues. FDOs can assist in lowering errors brought on by overlooked parameters when they are used to imitate real-world situations. They are also inextricably linked to memory-based systems, which are found in a large number of biological systems.



In order to effectively control the rice taungro virus, particularly in communities of control and infected individuals, and looked at rice taungro using a novel concept for control techniques. The creation of a new mathematical model for the recovery impact that incorporates early identification control mechanisms for rice taungro is the main objective of this project. A very deadly disease that poses a serious threat to plant life is rice taungro. An introduction and historical context will be given in Section 1 to aid readers in understanding the innovation. Along with control measures, a new mathematical model for the recovery effect under the suggested hypothesis will be created in section 2. Section 3 discusses equilibrium points with reproductive numbers as well as sensitivity and stability analyses. In section 4, analytical solutions that satisfy the proposed model’s positiveness, boundedness, and uniqueness are examined, and the global stability of the model at equilibrium and endemic points is also covered. In section 5, the Caputo operator with a power law kernel is used to construct numerical solutions, along with a stability analysis. MATLAB coding was used to do the simulation, with section 6 providing a detailed physical explanation and section 7 providing the final results.

**1.1. Preliminaries.** Review some of the basic concepts pertaining to fractional calculus results in this section. It will be carried out in the subsections that follow.

**Definition 1.1.** [20] Let  $K$  be the continuous based function on  $K^1([0, E], \mathcal{R})$ , so fractional order  $\eta \in (0, 1)$  of Riemann Liouville type integration is expressed as follows:

$${}^RGI_t^\eta K = \frac{1}{\Gamma(\eta)} \int_0^t (t - z)^{(\eta-1)} K(l) dl,$$

where the integral of right hand side is point to point from 0 to  $\infty$ .

**Definition 1.2.** [20] Let  $K$  be the continuous based function on  $K^1([0, E], \mathcal{R})$ , so following is the definition of  $K$ ’s Caputo derivative:

$${}^CI_t^\eta K = \frac{1}{\Gamma(n - \eta)} \left[ \int_0^t (t - l)^{(n-\eta-1)} \frac{d^n}{dl^n} K(l) dl \right], \tag{1.1}$$

where the Gamma function is denoted by  $\Gamma(\cdot)$ . Equation (1.1) reduces to when  $n = 1$ .

$${}^CI_t^\eta K = \frac{1}{\Gamma(n - \eta)} \left[ \int_0^t (t - l)^{(-\eta)} K'(l) dl \right].$$

**Lemma 1.3.** *The fixed position  $f^*$  is believed to symbolize the point of equilibrium of the Caputo model.*

$${}^CI_t^\eta K = K(t, f(t)), \quad 0 \leq \eta \leq 1,$$

if one and if only for each  $t$ ,  $f^*(t) = 0$ .

## 2. FORMULATION OF RICE TAUNGRO DISEASE MODEL

In order to maintain a healthy environment, this novel model for researching rice tungro disease offers several metrics for various consequences and early detection of diseased plants produced by stunted growth rice tungro disease. To the best of knowledge, no author has developed a model similar to the framework which devised, but a new model for rice tungro takes into account the many impacts. Assume that there are four classes within the plant population in this new model. The generative phase populations of susceptible rice plants are represented by  $S_g$ , the generative phase populations of infected rice plants by  $I_g$ , in the vegetative phase, the number of healthy rice plants is represented by  $S_h$ , whereas the number of infected rice plants is represented by  $I_h$ . Vulnerable vectors ( $S_v$ ) and infected vectors ( $I_v$ ) make up the two kinds of vectors. The population kinds that were observed included plants, vectors of illness, and carnivores.  $P$ .

Several parameters can be used to characterize the pace of change for healthy rice plants throughout the vegetative period.  $\phi_h$  is a representation of the birth rate of healthy rice plants in this phase. The infection rate, which refers to the transfer of infection from vectors to healthy rice plants, is denoted as  $\beta_1$ . Furthermore,  $\alpha_h$  indicates the natural



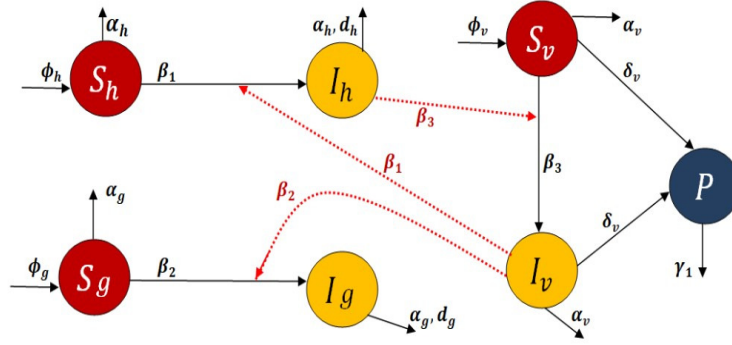


FIGURE 1. The newly created model is shown in the flow chart.

death rate of healthy rice plants throughout the vegetative period. The following formula represents the change in the number of healthy rice plants based on these parameters:

$$DS_h = \phi_h - \beta_1 S_h I_v - \alpha_h S_h.$$

Taking into consideration births, diseases, and natural deaths, this equation describes the dynamics of healthy rice plants during their vegetative period.

The rate of change for rice infected plants in the growing phase can be described as follows: The infection rate from healthy rice plants to infected rice plants in this phase is denoted by  $\beta_1$ . The natural death rate of infected rice plants is represented by  $\alpha_h$ , and the infection-related death rate for these plants is  $d_h$ . The equation governing this process is given by:

$$DI_h = \beta_1 S_h I_v - (\alpha_h + d_h) I_h.$$

Here,  $DI_h$  represents the change in the number of infected rice plants.

Several parameters can be used to represent how quickly healthy rice plants change throughout the generative period.  $\phi_g$  represents the birth rate of healthy rice plants in this phase. The infection rate from infected vectors affecting healthy rice plants is represented by  $\beta_2$ ; this describes the transition of healthy rice plants to infected ones. Furthermore,  $\alpha_g$  represents the natural death rate of healthy rice plants throughout the generative phase. The equation describing these dynamics is:

$$DS_g = \phi_g - \beta_2 S_g I_v - \alpha_g S_g.$$

Here,  $DS_g$  represents the change in the healthy rice plant population  $S_g$ .

The rate of change in infected rice plants during the generative phase is influenced by several factors. The infection rate caused by infected vectors moving from healthy rice plants to infected rice plants is denoted as  $\beta_2$ . Additionally, the natural death rate of infected rice plants in this phase is represented by  $\alpha_g$ , while the infection-related death rate is indicated as  $d_g$ . The resulting equation can be expressed as:

$$DI_g = \beta_2 S_g I_v - (\alpha_g + d_g) I_g.$$

The dynamics of infection and death in infected rice plants during their generative period are described by this equation.

For the rate of change in vulnerable vectors, and consider the following factors:

1. The birth rate of vulnerable vectors, denoted as  $\phi_v$ .
2. The infection rate from infected rice plants to vulnerable vectors, represented by  $\beta_3$ .
3. The natural death rate of vulnerable vectors, indicated by  $\alpha_v$ .
4. The transfer rate from vulnerable vectors to disease-carrying vectors and predators, denoted as  $\delta_v$ .

Taking these elements into account, the equation can be represented as:



$$DS_v = \phi_v - \beta_3 S_v I_h - (\alpha_v + \delta_v) S_v.$$

This equation describes the dynamic behavior of vulnerable vector populations in the presence of these factors.

The rate of change in vulnerable vectors is influenced by several factors. The birth rate of vulnerable vectors is denoted as  $\phi_v$ . The infection rate, which occurs when infected rice plants affect vulnerable vectors, is represented by  $\beta_3$ . Additionally, the natural death rate of vulnerable vectors is  $\alpha_v$ , while the transfer rate from vulnerable vectors to disease-carrying vectors and predators,  $P$ , is denoted as  $\delta_v$ .

Combining these factors, the equation for the dynamics of vulnerable vectors is expressed as:

$$DS_v = \phi_v - \beta_3 S_v I_h - (\alpha_v + \delta_v) S_v.$$

The rate of change of disease-carrying vectors and predators, denoted as  $P$ , can be described by the following equation:

The transfer rate from vulnerable vectors and infected vectors to the population of disease-carrying vectors and predators is represented by  $\delta_v$ . Additionally, the natural decay rate of disease-carrying vectors and predators is given by  $\gamma_1$ . As a result, the equation can be expressed as:

$$\frac{dP}{dt} = \delta_v(S_v + I_v) - \gamma_1 P.$$

This equation shows how the populations of disease-carrying vectors and predators change over time.

Consequently, the differential equations system has been represented using a flow chart 1, along with proposed hypothesis, illustrating an epidemic model with nonlinear incidence and a host vector.

$$\begin{aligned} DS_h &= \phi_h - \beta_1 S_h I_v - \alpha_h S_h; \\ DI_h &= \beta_1 S_h I_v - (\alpha_h + d_h) I_h; \\ DS_g &= \phi_g - \beta_2 S_g I_v - \alpha_g S_g; \\ DI_g &= \beta_2 S_g I_v - (\alpha_g + d_g) I_g; \\ DS_v &= \phi_v - \beta_3 S_v I_h - (\alpha_v + \delta_v) S_v; \\ DI_v &= \beta_3 S_v I_h - (\alpha_v + \delta_v) I_v; \\ DP &= \delta_v(S_v + I_v) - \gamma_1 P, \end{aligned} \tag{2.1}$$

with the following initial conditions:  $S_h(0) = S_h^0, I_h(0) = I_h^0, S_g(0) = S_g^0, I_g(0) = I_g^0, S_v(0) = S_v^0, I_v(0) = I_v^0, P(0) = P^0$ .

**2.1. Rice taungro virus model with fractional derivative.** The expansions of conventional integration order equations with a derivative that ranges from 0 to 1 is fractional order systems, covering a wider spectrum of real systems. Here, extend and modify the rice taungro transmission model (2.1) through an arrangement of not linear fractional order equations in the form of the Caputo derivative:

$$\begin{aligned} {}_0^C D_t^\eta S_h &= \phi_h - \beta_1 S_h I_v - \alpha_h S_h; \\ {}_0^C D_t^\eta I_h &= \beta_1 S_h I_v - (\alpha_h + d_h) I_h; \\ {}_0^C D_t^\eta S_g &= \phi_g - \beta_2 S_g I_v - \alpha_g S_g; \\ {}_0^C D_t^\eta I_g &= \beta_2 S_g I_v - (\alpha_g + d_g) I_g; \\ {}_0^C D_t^\eta S_v &= \phi_v - \beta_3 S_v I_h - (\alpha_v + \delta_v) S_v; \\ {}_0^C D_t^\eta I_v &= \beta_3 S_v I_h - (\alpha_v + \delta_v) I_v; \\ {}_0^C D_t^\eta P &= \delta_v(S_v + I_v) - \gamma_1 P, \end{aligned} \tag{2.2}$$

under the first circumstances listed below:  $S_h(0) = S_h^0, I_h(0) = I_h^0, S_g(0) = S_g^0, I_g(0) = I_g^0, S_v(0) = S_v^0, I_v(0) = I_v^0, P(0) = P^0$ .



### 3. EQUILIBRIUM POINTS AND REPRODUCTIVE NUMBER OF MODEL

In this part of the paper, an extensive overview of equilibrium points is given. To obtain these equilibrium locations, it is imperative to set the left side of Eq. (2.1) to zero, as illustrated below:

$$\begin{aligned}
0 &= \phi_h - \beta_1 S_h I_v - \alpha_h S_h; \\
0 &= \beta_1 S_h I_v - (\alpha_h + d_h) I_h; \\
0 &= \phi_g - \beta_2 S_g I_v - \alpha_g S_g; \\
0 &= \beta_2 S_g I_v - (\alpha_g + d_g) I_g; \\
0 &= \phi_v - \beta_3 S_v I_h - (\alpha_v + \delta_v) S_v; \\
0 &= \beta_3 S_v I_h - (\alpha_v + \delta_v) I_v; \\
0 &= \delta_v (S_v + I_v) - \gamma_1 P.
\end{aligned}$$

After simplification, get

$$\begin{aligned}
\phi_h &= (\beta_1 I_v + \alpha_h) S_h; \\
\beta_1 S_h I_v &= (\alpha_h + d_h) I_h; \\
\phi_g &= (\beta_2 I_v + \alpha_g) S_g; \\
\beta_2 S_g I_v &= (\alpha_g + d_g) I_g; \\
\phi_v &= (\beta_3 I_h + (\alpha_v + \delta_v)) S_v; \\
\beta_3 S_v I_h &= (\alpha_v + \delta_v) I_v; \\
\delta_v (S_v + I_v) &= \gamma_1 P.
\end{aligned}$$

The point of equilibrium in this model that is free of sickness with absence pythagoreans:

$$E_0 = \left\{ S_h = \frac{\phi_h}{\alpha_h}, I_h = 0, S_g = \frac{\phi_g}{\alpha_g}, I_g = 0, S_v = \frac{\phi_v}{\alpha_v + \delta_v}, I_v = 0, P = 0 \right\},$$

The point of equilibrium in this model that is free of sickness:

$$E_1 = \left\{ S_h = \frac{\phi_h}{\alpha_h}, I_h = 0, S_g = \frac{\phi_g}{\alpha_g}, I_g = 0, S_v = \frac{\phi_v}{\alpha_v + \delta_v}, I_v = 0, P = \frac{\delta_v \phi_v}{\gamma_1 (\alpha_v + \delta_v)} \right\},$$

as well as endemic points are  $E^* = (S_h^*, I_h^*, S_g^*, I_g^*, S_v^*, I_v^*, P^*)$  where

$$\begin{aligned}
S_h^* &= \frac{(\alpha_v + \delta_v) ((d_h + \alpha_h) (\alpha_v + \delta_v) + \beta_3 \phi_h)}{\beta_3 (\alpha_h (\alpha_v + \delta_v) + \beta_1 \phi_v)}; & I_h^* &= \frac{\beta_1 \beta_3 \phi_h \phi_v - \alpha_h (d_h + \alpha_h) (\alpha_v + \delta_v)^2}{\beta_3 (d_h + \alpha_h) (\alpha_h (\alpha_v + \delta_v) + \beta_1 \phi_v)}; \\
S_g^* &= \frac{\beta_1 \phi_g (\alpha_v + \delta_v) ((d_h + \alpha_h) (\alpha_v + \delta_v) + \beta_3 \phi_h)}{d_h (\alpha_v + \delta_v)^2 (\beta_1 \alpha_g - \beta_2 \alpha_h) + (\alpha_v + \delta_v) (\beta_1 \beta_3 \alpha_g \phi_h + \alpha_h (\alpha_v + \delta_v) (\beta_1 \alpha_g - \beta_2 \alpha_h)) + \beta_1 \beta_2 \beta_3 \phi_h \phi_v}; \\
I_g^* &= -\frac{\beta_2 \phi_g (\alpha_h (d_h + \alpha_h) (\alpha_v + \delta_v)^2 - \beta_1 \beta_3 \phi_h \phi_v)}{(d_g + \alpha_g) (d_h (\alpha_v + \delta_v)^2 (\beta_1 \alpha_g - \beta_2 \alpha_h) + (\alpha_v + \delta_v) A_1 + \beta_1 \beta_2 \beta_3 \phi_h \phi_v)}; \\
S_v^* &= \frac{(d_h + \alpha_h) (\alpha_h (\alpha_v + \delta_v) + \beta_1 \phi_v)}{\beta_1 ((d_h + \alpha_h) (\alpha_v + \delta_v) + \beta_3 \phi_h)}; & I_v^* &= \frac{\beta_1 \beta_3 \phi_h \phi_v - \alpha_h (d_h + \alpha_h) (\alpha_v + \delta_v)^2}{\beta_1 (\alpha_v + \delta_v) ((d_h + \alpha_h) (\alpha_v + \delta_v) + \beta_3 \phi_h)}; \\
P^* &= \frac{\delta_v \phi_v}{\gamma_1 (\alpha_v + \delta_v)},
\end{aligned}$$

where  $A_1 = (\beta_1 \beta_3 \alpha_g \phi_h + \alpha_h (\alpha_v + \delta_v) (\beta_1 \alpha_g - \beta_2 \alpha_h))$ . If the equilibrium position of the suggested model is asymptotically stable for each delay, it is deemed absolutely stable; if not, it is deemed condition safe for some durations but not throughout all durations.



**3.1. Reproduction number.** The Jacobian matrices  $F$  and  $V$ , which represent the functions  $F$  and  $V$  respectively, are analyzed at the equilibrium point free of infection, denoted as  $E_1$ . In matrix  $F$ , the element at position  $(i, j)$  indicates the rate at which a virus infected in compartment  $j$  spreads to compartment  $i$ . Similarly, the element at position  $(i, j)$  in matrix  $V$  reflects the spread of an existing infection.

To determine the reproduction number, and can use the spectral radius of the matrix  $FV^{-1}$  at the equilibrium point where there is no infection. This calculation follows the Next Generation Approach, which is explained as follows.

$$J_0 = \begin{pmatrix} -\alpha_h & 0 & 0 & 0 & 0 & -\frac{\beta_1 \phi_h}{\alpha_h} & 0 \\ 0 & -d_h - \alpha_h & 0 & 0 & 0 & \frac{\beta_1 \phi_h}{\alpha_h} & 0 \\ 0 & 0 & -\alpha_g & 0 & 0 & -\frac{\beta_2 \phi_g}{\alpha_g} & 0 \\ 0 & 0 & 0 & -d_g - \alpha_g & 0 & \frac{\beta_2 \phi_g}{\alpha_g} & 0 \\ 0 & -\frac{\beta_3 \phi_v}{\alpha_v + \delta_v} & 0 & 0 & -\alpha_v - \delta_v & 0 & 0 \\ 0 & \frac{\beta_3 \phi_v}{\alpha_v + \delta_v} & 0 & 0 & 0 & -\alpha_v - \delta_v & 0 \\ 0 & 0 & 0 & 0 & \delta_v & \delta_v & -\gamma_1 \end{pmatrix},$$

$J_0 = F - V.$

And constructed model's vectors  $F$  and  $V$  may be found with the help of Equation (2.1).

$$F = \begin{pmatrix} 0 & 0 & 0 & 0 & 0 & 0 & 0 \\ 0 & 0 & 0 & 0 & 0 & \frac{\beta_1 \phi_h}{\alpha_h} & 0 \\ 0 & 0 & 0 & 0 & 0 & 0 & 0 \\ 0 & 0 & 0 & 0 & 0 & \frac{\beta_2 \phi_g}{\alpha_g} & 0 \\ 0 & 0 & 0 & 0 & 0 & 0 & 0 \\ 0 & \frac{\beta_3 \phi_v}{\alpha_v + \delta_v} & 0 & 0 & 0 & 0 & 0 \\ 0 & 0 & 0 & 0 & \delta_v & \delta_v & 0 \end{pmatrix},$$

$$V = \begin{pmatrix} \alpha_h & 0 & 0 & 0 & 0 & \frac{\beta_1 \phi_h}{\alpha_h} & 0 \\ 0 & d_h + \alpha_h & 0 & 0 & 0 & 0 & 0 \\ 0 & 0 & \alpha_g & 0 & 0 & \frac{\beta_2 \phi_g}{\alpha_g} & 0 \\ 0 & 0 & 0 & d_g + \alpha_g & 0 & 0 & 0 \\ 0 & \frac{\beta_3 \phi_v}{\alpha_v + \delta_v} & 0 & 0 & \alpha_v + \delta_v & 0 & 0 \\ 0 & 0 & 0 & 0 & 0 & \alpha_v + \delta_v & 0 \\ 0 & 0 & 0 & 0 & 0 & 0 & \gamma_1 \end{pmatrix},$$

$$V^{-1} = \begin{pmatrix} \frac{\alpha_g \delta_v + \alpha_g \alpha_v}{\alpha_g \alpha_h \delta_v + \alpha_g \alpha_h \alpha_v} & 0 & 0 & 0 & 0 & -\frac{\beta_1 \alpha_g \phi_h}{\alpha_h (\alpha_g \alpha_h \delta_v + \alpha_g \alpha_h \alpha_v)} & 0 \\ 0 & \frac{1}{d_h + \alpha_h} & 0 & 0 & 0 & 0 & 0 \\ 0 & 0 & \frac{\alpha_h \delta_v + \alpha_h \alpha_v}{\alpha_g \alpha_h \delta_v + \alpha_g \alpha_h \alpha_v} & 0 & 0 & -\frac{\beta_2 \phi_g \alpha_h}{\alpha_g (\alpha_g \alpha_h \delta_v + \alpha_g \alpha_h \alpha_v)} & 0 \\ 0 & 0 & 0 & \frac{1}{d_g + \alpha_g} & 0 & 0 & 0 \\ 0 & -\frac{\beta_3 \phi_v}{(d_h + \alpha_h)(\alpha_v + \delta_v)^2} & 0 & 0 & \frac{1}{\alpha_v + \delta_v} & 0 & 0 \\ 0 & 0 & 0 & 0 & 0 & \frac{\alpha_g \alpha_h}{\alpha_g \alpha_h \delta_v + \alpha_g \alpha_h \alpha_v} & 0 \\ 0 & 0 & 0 & 0 & 0 & 0 & \frac{1}{\gamma_1} \end{pmatrix},$$

$K = F.V^{-1}.$



So,

$$K = \begin{pmatrix} 0 & 0 & 0 & 0 & 0 & 0 \\ 0 & 0 & 0 & 0 & \frac{\beta_1 \alpha_g \phi_h}{\alpha_g \alpha_h \delta_v + \alpha_g \alpha_h \alpha_v} & 0 \\ 0 & 0 & 0 & 0 & 0 & 0 \\ 0 & 0 & 0 & 0 & \frac{\beta_2 \phi_g \alpha_h}{\alpha_g \alpha_h \delta_v + \alpha_g \alpha_h \alpha_v} & 0 \\ 0 & 0 & 0 & 0 & 0 & 0 \\ 0 & \frac{\beta_3 \phi_v}{(d_h + \alpha_h)(\alpha_v + \delta_v)} & 0 & 0 & 0 & 0 \\ 0 & -\frac{\beta_3 \delta_v \phi_v}{(d_h + \alpha_h)(\alpha_v + \delta_v)^2} & 0 & 0 & \frac{\delta_v}{\alpha_v + \delta_v} & \frac{\alpha_g \alpha_h \delta_v}{\alpha_g \alpha_h \delta_v + \alpha_g \alpha_h \alpha_v} \end{pmatrix}.$$

Thus

$$|K - \Upsilon I| = 0,$$

$$\begin{vmatrix} -\Upsilon & 0 & 0 & 0 & 0 & 0 & 0 \\ 0 & -\Upsilon & 0 & 0 & 0 & \frac{\beta_1 \alpha_g \phi_h}{\alpha_g \alpha_h \delta_v + \alpha_g \alpha_h \alpha_v} & 0 \\ 0 & 0 & -\Upsilon & 0 & 0 & 0 & 0 \\ 0 & 0 & 0 & -\Upsilon & 0 & \frac{\beta_2 \phi_g \alpha_h}{\alpha_g \alpha_h \delta_v + \alpha_g \alpha_h \alpha_v} & 0 \\ 0 & 0 & 0 & 0 & -\Upsilon & 0 & 0 \\ 0 & \frac{\beta_3 \phi_v}{(d_h + \alpha_h)(\alpha_v + \delta_v)} & 0 & 0 & 0 & -\Upsilon & 0 \\ 0 & -\frac{\beta_3 \delta_v \phi_v}{(d_h + \alpha_h)(\alpha_v + \delta_v)^2} & 0 & 0 & \frac{\delta_v}{\alpha_v + \delta_v} & \frac{\alpha_g \alpha_h \delta_v}{\alpha_g \alpha_h \delta_v + \alpha_g \alpha_h \alpha_v} & -\Upsilon \end{vmatrix} = 0.$$

Following the solution of the eigenvalue matrix above, obtain the  $\Upsilon$  as following.

$$\Upsilon = \frac{\sqrt{\beta_1} \sqrt{\beta_3} \sqrt{\phi_h} \sqrt{\phi_v}}{\sqrt{\alpha_h} \sqrt{d_h + \alpha_h} (\alpha_v + \delta_v)}.$$

Given that the dominating eigenvalue of the matrix  $FV^{-1}$  is linked to the reproductive number  $R_0$ , as shown by:

$$R_0 = \frac{\sqrt{\beta_1} \sqrt{\beta_3} \sqrt{\phi_h} \sqrt{\phi_v}}{\sqrt{\alpha_h} \sqrt{d_h + \alpha_h} (\alpha_v + \delta_v)}.$$

**3.2. Sensitivity Analysis.** Sensitivity analysis is helpful for comprehending how various circumstances affect a model's stability, particularly when they involve unclear data. It also aids in determining crucial process factors. For example, and can evaluate the sensitivity of  $R_0$  as follows by computing the partial derivatives of the threshold with regard to pertinent parameters:

$$\frac{\partial R_0}{\partial \beta_1} = \frac{\sqrt{\beta_3} \sqrt{\phi_h} \sqrt{\phi_v}}{2\sqrt{\beta_1} \sqrt{\alpha_h} \sqrt{d_h + \alpha_h} (\alpha_v + \delta_v)} > 0,$$

$$\frac{\partial R_0}{\partial \beta_3} = \frac{\sqrt{\beta_1} \sqrt{\phi_h} \sqrt{\phi_v}}{2\sqrt{\beta_3} \sqrt{\alpha_h} \sqrt{d_h + \alpha_h} (\alpha_v + \delta_v)} > 0, \quad \frac{\partial R_0}{\partial \phi_h} = \frac{\sqrt{\beta_1} \sqrt{\beta_3} \sqrt{\phi_v}}{2\sqrt{\alpha_h} \sqrt{\phi_h} \sqrt{d_h + \alpha_h} (\alpha_v + \delta_v)} > 0,$$

$$\frac{\partial R_0}{\partial \phi_v} = \frac{\sqrt{\beta_1} \sqrt{\beta_3} \sqrt{\phi_h}}{2\sqrt{\alpha_h} \sqrt{\phi_v} \sqrt{d_h + \alpha_h} (\alpha_v + \delta_v)} > 0;$$

$$\frac{\partial R_0}{\partial \alpha_h} = -\frac{\sqrt{\beta_1} \sqrt{\beta_3} \sqrt{\phi_h} \sqrt{\phi_v}}{2\alpha_h^{3/2} \sqrt{d_h + \alpha_h} (\alpha_v + \delta_v)} - \frac{\sqrt{\beta_1} \sqrt{\beta_3} \sqrt{\phi_h} \sqrt{\phi_v}}{2\sqrt{\alpha_h} (d_h + \alpha_h)^{3/2} (\alpha_v + \delta_v)} < 0,$$

$$\frac{\partial R_0}{\partial \alpha_v} = -\frac{\sqrt{\beta_1} \sqrt{\beta_3} \sqrt{\phi_h} \sqrt{\phi_v}}{\sqrt{\alpha_h} \sqrt{d_h + \alpha_h} (\alpha_v + \delta_v)^2} < 0, \quad \frac{\partial R_0}{\partial \delta_v} = -\frac{\sqrt{\beta_1} \sqrt{\beta_3} \sqrt{\phi_h} \sqrt{\phi_v}}{\sqrt{\alpha_h} \sqrt{d_h + \alpha_h} (\alpha_v + \delta_v)^2} < 0,$$

$$\frac{\partial R_0}{\partial d_h} = -\frac{\sqrt{\beta_1} \sqrt{\beta_3} \sqrt{\phi_h} \sqrt{\phi_v}}{2\sqrt{\alpha_h} (d_h + \alpha_h)^{3/2} (\alpha_v + \delta_v)} < 0.$$



Parameters	$\beta_1$	$\beta_3$	$\phi_h$	$\phi_v$	$\alpha_h$	$\alpha_v$	$\delta_v$	$d_h$
Sensitivity Values	5.93171	1.56098	0.158179	2.37268	-3.8373	-0.474537	-0.474537	-1.46462

It's important to remember that adjusting the settings can significantly impact the value of  $R_0$ . In study, parameters like  $\beta_1, \beta_3, \phi_h$ , and  $\phi_v$  represent expansion, while  $\alpha_h, \alpha_v, \delta_v$ , and  $d_h$  signify contraction. Therefore, it's essential to prioritize prevention over therapy for effective infection control see in Figure 2, 3, and 4.

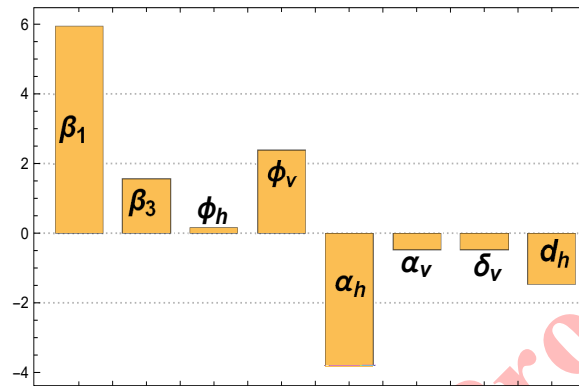


FIGURE 2. Analysis of  $R_0$  sensitivity using various parameters.

It is evident from all of the aforementioned sub-figures that the value of  $R_0$  is very responsive in terms of how its rate of change behaves. The behavior of  $R_0$  w.r.t  $\beta_1$  &  $\beta_3$ ,  $\beta_3$  &  $\phi_h$ , and  $\phi_h$  &  $\phi_v$  is approximately similar with minor effects at these parameters. Similarly the behavior of  $R_0$  w.r.t  $\alpha_h$  &  $\phi_v$ ,  $\alpha_v$  &  $d_h$ , and  $\delta_v$  &  $\beta_1$  approximately same behavior with some minor effects. Furthermore, the behavior of  $R_0$  w.r.t  $\delta_v$  &  $\alpha_v$  and  $d_h$  &  $\alpha_h$  having approximately different behaviour with minor effects. However, each sub-figure shows that each parameter's rate of change is bounded, which is necessary for stable conditions.

#### 4. ANALYSIS OF MODEL

**4.1. Unique solution and Positiveness.** When  $\eta \rightarrow 1$ , the model (2.2) simplifies to an integer-order model. Additionally, the system (2.2) has the initial state  $S_h(0) = S_h^0, I_h(0) = I_h^0, S_g(0) = S_g^0, I_g(0) = I_g^0, I_v(0) = I_v^0, P(0) = P^0$ , and  $S_v(0) = S_v^0$ .

One way to express the model (2.2) is as

$${}^C D_t^\eta H(t) = K(H(t)), \quad t \in (0, T], \quad H(0) = H^0, \tag{4.1}$$

where

$$H = \begin{pmatrix} S_h \\ I_h \\ S_g \\ I_g \\ S_v \\ I_v \\ P \end{pmatrix}, \quad H(0) = \begin{pmatrix} S_h(0) \\ I_h(0) \\ S_g(0) \\ I_g(0) \\ S_v(0) \\ I_v(0) \\ P(0) \end{pmatrix}, \quad K(H) = \begin{pmatrix} \phi_h - \beta_1 S_h I_v - \alpha_h S_h \\ \beta_1 S_h I_v - (\alpha_h + d_h) I_h \\ \phi_g - \beta_2 S_g I_v - \alpha_g S_g \\ \beta_2 S_g I_v - (\alpha_g + d_g) I_g \\ \phi_v - \beta_3 S_v I_h - (\alpha_v + \delta_v) S_v \\ \beta_3 S_v I_h - (\alpha_v + \delta_v) I_v \\ \delta_v (S_v + I_v) - \gamma_1 P \end{pmatrix}.$$

Define a supremum norm for  $K$  as

$$\|K\| = \sup_{t \in (0, T]} |K(t)|,$$

and define a norm as

$$\|C\| = \sum_{i,j} \sup_{t \in (0, T]} |c_{ij}(t)|.$$



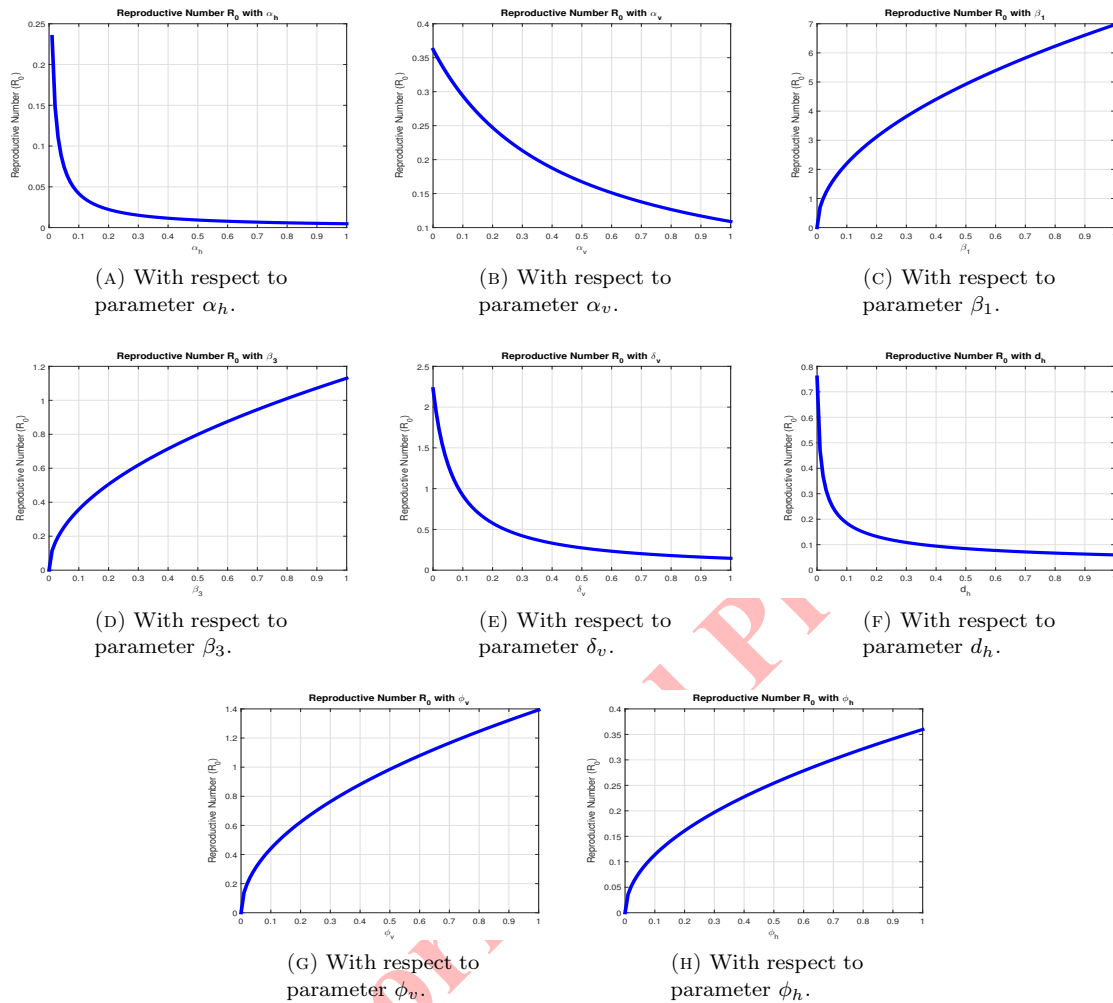


FIGURE 3. Reproductive graph with different parameters.

For the matrix  $C = [C_{ij}(t)]$ .

The solution of the system (4.1) now takes the following form based on the definition of the Caputo fractional derivative (1.1):

$$H(t) = H^0 + \frac{1}{\Gamma(\eta)} \int_0^t (t-p)^{\eta-1} F(H(p)) dp = \Psi(H).$$

This gives the equality

$$\Psi(H_1) - \Psi(H_2) = \frac{1}{\Gamma(\eta)} \int_0^t (t-p)^{\eta-1} (K(H_1(p)) - K(H_2(p))) dp.$$



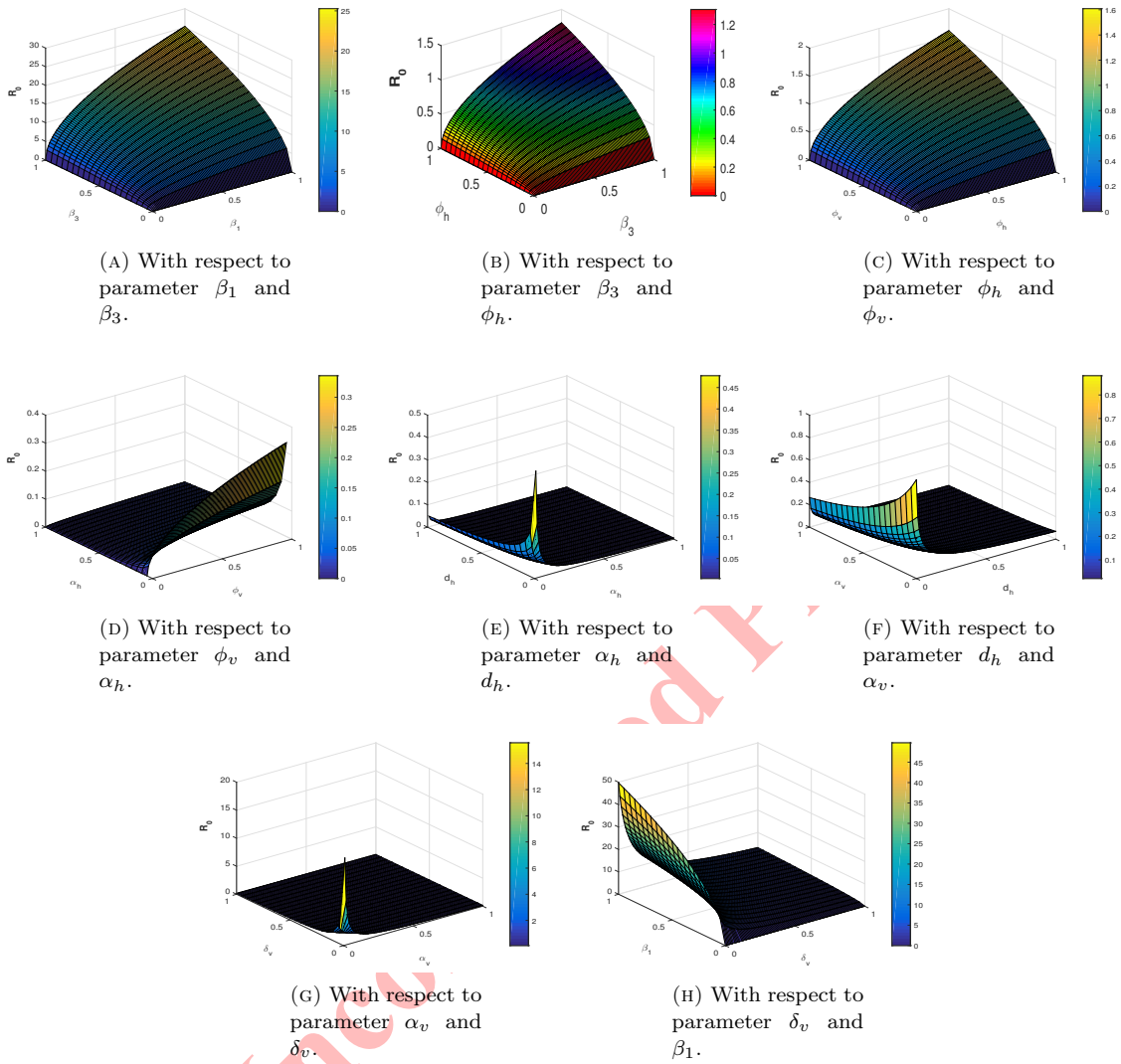


FIGURE 4. Sensitivity Graphs with different parameters.

Hence having

$$\begin{aligned}
 \|\Psi(H_1) - \Psi(H_2)\| &= \frac{1}{\Gamma(\eta)} \left\| \int_0^t (t-p)^{\eta-1} (K(H_1(p)) - K(H_2(p))) dp \right\| \\
 &\leq \frac{1}{\Gamma(\eta)} \int_0^t (t-p)^{\eta-1} \|K(H_1(p)) - K(H_2(p))\| dp \\
 &\leq \psi \|H_1 - H_2\| dp,
 \end{aligned}$$



where

$$\psi = M^\eta \max \{(\alpha_h + \beta_1 \xi), (\alpha_h + d_h), (\alpha_g + \beta_2 \xi), (\alpha_g + d_g), (\alpha_v + \delta_v + \beta_3 \xi), (\alpha_v + \delta_v), \gamma_1\},$$

$$M^\eta = \frac{T^\eta}{\Gamma(\eta + 1)},$$

and  $\Lambda = \{(S_h, I_h, S_g, I_g, S_v, I_v, P) : \max(|S_h|, |I_h|, |S_g|, |I_g|, |S_v|, |I_v|, |P|)\} \leq \xi$ .

Thus, if the mapping  $\Psi(H)$  is a contraction mapping, that is, if  $\psi < 1$ , then there is a unique solution for the system (4.1). Consequently, arrive at the following conclusion:

**Theorem 4.1.** *The region  $\Lambda \times (0, T]$  contains a unique solution for the system (4.1) corresponding to the initial condition  $K(0) = K^0$ . Where  $t \in (0, T]$ ,  $\Lambda = \{(S_h, I_h, S_g, I_g, S_v, I_v, P) : \max(|S_h|, |I_h|, |S_g|, |I_g|, |S_v|, |I_v|, |P|)\} \leq \xi$ , if*

$$\psi = M^\eta \max \{(\alpha_h + \beta_1 \xi), (\alpha_h + d_h), (\alpha_g + \beta_2 \xi), (\alpha_g + d_g), (\alpha_v + \delta_v + \beta_3 \xi), (\alpha_v + \delta_v), \gamma_1\} < 1,$$

where  $M^\eta = \frac{T^\eta}{\Gamma(\eta+1)}$ .

Again, it is clear that

$$\left\{ \begin{array}{ll} \begin{array}{l} {}_0^C D_t^\eta S_h|_{S_h=0} = \phi_h, \\ {}_0^C D_t^\eta I_h|_{I_h=0} = \beta_1 S_h I_v, \end{array} & \text{where } S_h, I_v \geq 0; \\ \begin{array}{l} {}_0^C D_t^\eta S_g|_{S_g=0} = \phi_g, \\ {}_0^C D_t^\eta I_g|_{I_g=0} = \beta_2 S_g I_v, \end{array} & \text{where } S_g, I_v \geq 0; \\ \begin{array}{l} {}_0^C D_t^\eta S_v|_{S_v=0} = \phi_v, \\ {}_0^C D_t^\eta I_v|_{I_v=0} = \beta_3 S_v I_h, \end{array} & \text{where } S_v, I_h \geq 0; \\ {}_0^C D_t^\eta P|_{P=0} = \delta_v (S_v + I_v), & \text{where } S_v, I_v \geq 0. \end{array} \right. \quad (4.2)$$

Thus, the vector field points into  $\mathbb{R}_7^+$  on each plane that borders the non-negative octant. Consequently,  $\mathbb{R}_7^+$  will continue to contain the answer. As a result, say the following:

**Theorem 4.2.** *Every solution for the fractional-order system under consideration (2.2) stays in  $\mathbb{R}_7^+$ .*

#### 4.2. Bounded-ness with positive invariant region.

**Theorem 4.3.** *The model's solutions (2.2) are invariant over nonnegative real numbers in the region  $\Phi$  proper subset of seven-dimensional space, meaning that*

$$\Phi = \left\{ (S_h, I_h, S_g, I_g, S_v, I_v, P) : Q_h = S_h + I_h \leq \frac{\phi_h}{\alpha_h}, Q_g = S_g + I_g \leq \frac{\phi_g}{\alpha_g}, Q_v = S_v + I_v \leq \frac{\phi_v}{(\alpha_v + \delta_v)}, \right.$$

$$\left. Q_p = P \leq \frac{\delta_v Q_v}{\gamma_1} \right\}. \quad (4.3)$$

**Proof:** Use the technique to demonstrate the boundedness of the solution. Therefore, by adding matching terms to the left and right of the characteristics in the model (2.2), getting

$${}_0^C D_t^\eta Q_h = {}_0^C D_t^\eta S_h + {}_0^C D_t^\eta I_h = \phi_h - \alpha_h S_h - \alpha_h I_h - d_h I_h.$$

Implies

$${}_0^C D_t^\eta Q_h \leq \phi_h - \alpha_h Q_h.$$

Furthermore, reformulated the preceding expression to facilitate computation.

$${}_0^C D_t^\eta Q_h = \phi_h - \alpha_h Q_h.$$

Additionally, from the previous expression, getting

$${}_0^C D_t^\eta Q_h + \alpha_h Q_h = \phi_h.$$

The Laplace transform applied to both sides of the previous equation also produces

$$\mathcal{L}\{{}_0^C D_t^\eta Q_h\}(s) + \alpha_h \mathcal{L}\{Q_h\}(s) = \mathcal{L}\{\phi_h\}.$$



The previous equation reduces to the following form when the Laplace transform definition is used in the Caputo fractional derivative sense so that  $\mathfrak{L}\{Q_h\}(s) = \mathfrak{Q}_h(s) = \mathfrak{Q}_h$

$$s^\eta \mathfrak{Q}_h - \sum_{k=0}^{n-1} s^{\eta-k-1} Q_h^k(0) + \alpha_h \mathfrak{Q}_h = \frac{\phi_h}{s}.$$

Additionally, the above equation reduces to  $n = 1; 0 < \eta < 1$ .

$$s^\eta \mathfrak{Q}_h - \sum_{k=0}^0 s^{\eta-k-1} Q_h^k(0) + \alpha_h \mathfrak{Q}_h = \frac{\phi_h}{s}.$$

Additionally, using the summation condition, the above equation decreases to

$$s^\eta \mathfrak{Q}_h - s^{\eta-1} Q_h(0) + \alpha_h \mathfrak{Q}_h = \frac{\phi_h}{s}.$$

Additionally, the previous equation can be expressed as follows by rearranging the terms:

$$(s^\eta + \alpha_h) \mathfrak{Q}_h - s^{\eta-1} Q_h(0) = \frac{\phi_h}{s}.$$

Additionally, when  $\mathfrak{Q}_h$  is solved for, the previous equation reduces to

$$\mathfrak{Q}_h = \frac{\phi_h s^{-1}}{(s^\eta + \alpha_h)} + \frac{s^{\eta-1} Q_h(0)}{(s^\eta + \alpha_h)}.$$

Furthermore, by performing the inverse Laplace transform on both sides of the previous equation, and able to

$$\mathfrak{L}^{-1}\{\mathfrak{Q}_h\} = \mathfrak{L}^{-1}\left\{ \frac{\phi_h s^{-1}}{(s^\eta + \alpha_h)} + \frac{s^{\eta-1} Q_h(0)}{(s^\eta + \alpha_h)} \right\}.$$

Using the inverse Laplace transform property once more, the previous equation yields

$$\mathfrak{L}^{-1}\{\mathfrak{Q}_h\} = \phi_h \mathfrak{L}^{-1}\left\{ \frac{s^{-1}}{(s^\eta + \alpha_h)} \right\} + Q_h(0) \mathfrak{L}^{-1}\left\{ \frac{s^{\eta-1}}{(s^\eta + \alpha_h)} \right\}.$$

Additionally, utilizing the connection between the Mittag Leffler function and the inverse Laplace transform  $t^{\beta-1} E_{\eta,\beta}(\kappa t^\eta) = \mathfrak{L}^{-1}\{s^{\eta-\beta}/s^\eta - \kappa\}$ , the previous formula decreases to

$$Q_h(t) = \phi_h (t^{\eta+1-1} E_{\eta,\eta+1}(-\alpha_h t^\eta)) + Q_h(0) (t^{1-1} E_{\eta,1}(-\alpha_h t^\eta)).$$

Implies,

$$Q_h(t) = \phi_h t^\eta E_{\eta,\eta+1}(-\alpha_h t^\eta) + Q_h(0) E_{\eta,1}(-\alpha_h t^\eta).$$

Additionally, the Mittag Leffler function definition is  $E_{\eta,\eta+\beta}(g) = 1/g E_{\eta,\beta}(g) - 1/g\sqrt{\beta}$ . The equation that follows reduces to

$$Q_h(t) = \phi_h t^\eta \left( \frac{1}{-\alpha_h t^\eta} E_{\eta,1}(-\alpha_h t^\eta) - \frac{1}{-\alpha_h t^\eta \sqrt{1}} \right) + Q_h(0) E_{\eta,1}(-\alpha_h t^\eta).$$

Implies

$$Q_h(t) = \left( -\frac{\phi_h}{\alpha_h} E_{\eta,1}(-\alpha_h t^\eta) + \frac{\phi_h}{\alpha_h} \right) + Q_h(0) E_{\eta,1}(-\alpha_h t^\eta).$$

Consequently, if consider Equation (3), getting:

$$Q_h(t) = \frac{\phi_h}{\alpha_h} + \left( Q_h(0) - \frac{\phi_h}{\alpha_h} \right) E_{\eta,1}(-\alpha_h t^\eta).$$

Therefore, the size of the entire healthy population is bounded between 0 and  $\frac{\phi_h}{\alpha_h}$  as time  $t$  increases. Similarly for the total growing population size is bounded between 0 and  $\frac{\phi_g}{\alpha_g}$  and similarly for the total growing vector size is bounded between 0 and  $\frac{\phi_v}{\alpha_v + \delta_v}$ . At the end for the total pythagoreans population size is bounded between 0 and  $\frac{\delta_v Q_v}{\gamma_1}$ .



## 5. LOCAL STABILITY

Solve  $a$  to get the system's equilibrium points (2.2) in order to verify the system's stability. The system's three biologically viable equilibrium points (2.2) are shown in the subsections below, along with the accompanying stability analysis.

**5.1. Local Stability at trivial.** In this sense, consider  $S_h = I_h = S_g = I_g = S_v = I_v = P = 0$ . Assuming that there are no diseases in the plants, the bacteria do not spread while the plants are in activity. The disease-free trivial equilibrium is therefore determined to be  $E(0, 0, 0, 0, 0, 0, 0)$ , which is always present.

The system's Jacobian matrix (2.2) as assessed at the state of no sickness

$$J_0(E) = \begin{pmatrix} -\alpha_h & 0 & 0 & 0 & 0 & 0 & 0 \\ 0 & -d_h - \alpha_h & 0 & 0 & 0 & 0 & 0 \\ 0 & 0 & -\alpha_g & 0 & 0 & 0 & 0 \\ 0 & 0 & 0 & -d_g - \alpha_g & 0 & 0 & 0 \\ 0 & 0 & 0 & 0 & -\alpha_v - \delta_v & 0 & 0 \\ 0 & 0 & 0 & 0 & 0 & -\alpha_v - \delta_v & 0 \\ 0 & 0 & 0 & 0 & \delta_v & \delta_v & -\gamma_1 \end{pmatrix}.$$

The characteristics polynomials of  $J_0(E)$  is

$$(-\gamma_1 - k)(-\alpha_g - k)(-\alpha_h - k)(-d_g - \alpha_g - k)(-d_h - \alpha_h - k)(-k - \alpha_v - \delta_v)^2.$$

The eigenvalues of the matrix are

$$k_1 = -d_g - \alpha_g, k_2 = -\alpha_g, k_3 = -d_h - \alpha_h, k_4 = -\alpha_h, k_5 = -\gamma_1, k_6 = -\alpha_v - \delta_v, k_7 = -\alpha_v - \delta_v.$$

Can therefore express this outcome as follows:

**Theorem 5.1.** *There is always a disease-free trivial equilibrium  $E$ , and it behaves steadily.*

**5.2. Local Stability at  $E_0$ .** Suppose there are disease exists in the plants, but the bacterial do not transfers in the plants in action; thus, in this sense, take  $I_h = I_g = I_v = P = 0$ . The disease-free equilibrium points in the absence of bacteria are then determined to be  $E_0$ , which is always present.

The system's Jacobian matrix (2.2) was assessed at the disease-free equilibrium when there were no bacteria present.

$$J_0(E_0) = \begin{pmatrix} -\alpha_h & 0 & 0 & 0 & 0 & -\frac{\beta_1 \phi_h}{\alpha_h} & 0 \\ 0 & -d_h - \alpha_h & 0 & 0 & 0 & \frac{\beta_1 \phi_h}{\alpha_h} & 0 \\ 0 & 0 & -\alpha_g & 0 & 0 & -\frac{\beta_2 \phi_g}{\alpha_g} & 0 \\ 0 & 0 & 0 & -d_g - \alpha_g & 0 & \frac{\beta_2 \phi_g}{\alpha_g} & 0 \\ 0 & -\frac{\beta_3 \phi_v}{\alpha_v + \delta_v} & 0 & 0 & -\alpha_v - \delta_v & 0 & 0 \\ 0 & \frac{\beta_3 \phi_v}{\alpha_v + \delta_v} & 0 & 0 & 0 & -\alpha_v - \delta_v & 0 \\ 0 & 0 & 0 & 0 & \delta_v & \delta_v & -\gamma_1 \end{pmatrix}.$$

The characteristics polynomials of  $J_0(E_1)$  is

$$\frac{(-\gamma_1 - \lambda)(\alpha_g + \lambda)(\alpha_h + \lambda)(d_g + \alpha_g + \lambda)(\lambda + \alpha_v + \delta_v)(\alpha_h(\alpha_v + \delta_v)(d_h + \alpha_h + \lambda)(\lambda + \alpha_v + \delta_v) - \beta_1 \beta_3 \phi_h \phi_v)}{\alpha_h(\alpha_v + \delta_v)}.$$

The eigenvalues of the matrix are

$$\lambda_1 = -d_g - \alpha_g, \lambda_2 = -\alpha_g, \lambda_3 = -\alpha_h, \lambda_4 = -\gamma_1, \lambda_5 = -\alpha_v - \delta_v, \lambda_6 = \frac{1}{2(\alpha_h \delta_v + \alpha_h \alpha_v)}, \lambda_7 = \frac{1}{2(\alpha_h \delta_v + \alpha_h \alpha_v)}.$$

Thus, state the following theorem:

**Theorem 5.2.** *The disease-free equilibrium points with absence of bacterial  $E_0$  always exists and shows stable behavior; otherwise, it is unstable.*



TABLE 1. Stability of the system (2.2) around its equilibrium point.

Equilibrium Point	Eigenvalues	stability
$E(0,0,0,0,0,0)$	-0.122,-0.091,-0.036,-0.005,-0.021,-0.5,-0.5	stable
$E_0(122.549, 0, 5.49, 0, 0.1, 0, 2.047)$	-0.122, -0.091, -0.05, -0.021, -0.5, -0.505, -0.075	Stable
$E_1(122.549, 0, 5.49, 0, 0.1, 0, 2.047)$	-0.122, -0.091, -0.05, -0.021, -0.5, -0.505, -0.075	Stable
$E^*(122.44, 0.018, 5.49, 0.00012, 0.099, 0.00027, 2.047)$	-0.122, -0.091, -0.021, -0.5, -0.00095, -0.537, -0.00608	Stable

5.3. **Local Stability at  $E^*$ .** Suppose there are disease exists in the plants with the bacterial that transfers in the plants in action; thus, in this sense, take  $S_h = I_h = S_g = I_g = S_v = I_v = P \neq 0$ . The endemic points are then determined to be  $E^*$ , which is always present.

The system's Jacobian matrix (2.2) as assessed at the endemic sites

$$J_0(E^*) = \begin{pmatrix} -\beta_1 I_v^* - \alpha_h & 0 & 0 & 0 & 0 & -S_h^* \beta_1 & 0 \\ \beta_1 I_v^* & -d_h - \alpha_h & 0 & 0 & 0 & S_h^* \beta_1 & 0 \\ 0 & 0 & -\beta_2 I_v^* - \alpha_g & 0 & 0 & \beta_2 (-S_g^*) & 0 \\ 0 & 0 & \beta_2 I_v^* & -d_g - \alpha_g & 0 & \beta_2 S_g^* & 0 \\ 0 & \beta_3 (-S_v^*) & 0 & 0 & -\beta_3 I_h^* - \alpha_v - \delta_v & 0 & 0 \\ 0 & \beta_3 S_v^* & 0 & 0 & \beta_3 I_h^* & -\alpha_v - \delta_v & 0 \\ 0 & 0 & 0 & 0 & \delta_v & \delta_v & -\gamma_1 \end{pmatrix}.$$

The characteristics polynomials of  $J_0(E^*)$  is

$$(-\gamma_1 - l)(-d_g - \alpha_g - l)(-\beta_2 I_v^* - \alpha_g - l) \left( (-\beta_3 I_h^* - l - \alpha_v - \delta_v) \left( (-d_h - \alpha_h - l)(-l - \alpha_v - \delta_v) \right. \right. \\ \left. \left. (-\beta_1 I_v^* - \alpha_h - l) - \beta_3 e(-S_h^* \beta_1 \alpha_h - S_h^* \beta_1 l) \right) + \beta_3 S_v^* (S_h^* \beta_1 \beta_3 I_h^* \alpha_h + S_h^* \beta_1 \beta_3 I_h^* l) \right).$$

The eigenvalues of the matrix are

$$l_1 = -d_g - \alpha_g, l_2 = -\beta_2 I_v^* - \alpha_g, l_3 = -\gamma_1, l_4 = -\alpha_v - \delta_v, l_5 = \frac{1}{3}(-\beta_3 I_h^* - d_h - \beta_1 I_v^* - 2\alpha_h - \alpha_v - \delta_v), \\ l_6 = \frac{1}{3}(-\beta_3 I_h^* - d_h - \beta_1 I_v^* - 2\alpha_h - \alpha_v - \delta_v), l_7 = \frac{1}{3}(-\beta_3 I_h^* - d_h - \beta_1 I_v^* - 2\alpha_h - \alpha_v - \delta_v).$$

The Routh-Hurwitz criterion states that if all of the equations' roots are negative or have negative real portions, the system (2.2) is locally asymptotically stable. Therefore, the following theorem can be stated:

**Theorem 5.3.** *The endemic points  $E^*$  always exists and shows stable behavior; otherwise, it is unstable.*

5.4. **Stability of the system.** Based on the eigenvalues of the corresponding Jacobian of the system (2.2), demonstrate the stability of the system (2.2) around its equilibrium point in Table 1.

### 6. GLOBAL STABILITY ANALYSIS

Stable analysis of equilibrium locations, as defined by the Lyapunov functional, is an essential idea in control and systems theory. The following material explains how to examine the equilibrium points' long-term behavior in both linear and nonlinear systems without actually solving the differential equation. It describes the asymptotic stability of a positive definite function with a negative definite temporal derivative. Here, prove a key lemma [10] in order to investigate the global stability of the suggested system.

**Lemma 6.1.** *For any  $t \geq t_0$ , let us assume that  $M \in \mathbb{R}^+$  is a continuous function.*

$${}^C D_t^\eta \left( M - M^* - M^* \log \frac{M}{M^*} \right) \leq \left( 1 - \frac{M}{M^*} \right) {}^C D_t^\eta M(t),$$



$M^* \in \mathbb{R}^+, \forall \eta \in (0, 1)$ .

**Theorem 6.2.** *The global type asymptotic disease-free equilibrium position  $E_1$  is at a stable position if the reproduction number is not having value greater than 1.*

*Proof.* The evidence has already been demonstrated in [22].  $\square$

**Theorem 6.3.** *The function globally asymptotically stable at the points  $E_2$  of the endemic equilibrium when  $R_0 > 1$  which is the reproductive number.*

*Proof.* The proof is emit and already similar proof in [22].  $\square$

## 7. COMPUTATIONAL ANALYSIS WITH CAPUTO OPERATOR

The Caputo derivative, which depends on the power-law kernel, is recommended by the literature as a way to use power-law modeling for practical applications. Furthermore, by using a numerical technique based on Newton's polynomial interpolation and replacing the temporal derivatives with the Caputo derivative, power law effects from fractional mathematics can be included. Here, introduce a numerical approach to address the problem outlined in Equation (2.2), which is based on a Newton polynomial.

$$\begin{aligned} {}_0^C D_t^\eta S_h &= S_{h1}(t, S_h) = \phi_h - \beta_1 S_h I_v - \alpha_h S_h; \\ {}_0^C D_t^\eta I_h &= I_{h1}(t, I_h) = \beta_1 S_h I_v - (\alpha_h + d_h) I_h; \\ {}_0^C D_t^\eta S_g &= S_{g1}(t, S_g) = \phi_g - \beta_2 S_g I_v - \alpha_g S_g; \\ {}_0^C D_t^\eta I_g &= I_{g1}(t, I_g) = \beta_2 S_g I_v - (\alpha_g + d_g) I_g; \\ {}_0^C D_t^\eta S_v &= S_{v1}(t, S_v) = \phi_v - \beta_3 S_v I_h - (\alpha_v + \delta_v) S_v; \\ {}_0^C D_t^\eta I_v &= I_{v1}(t, I_v) = \beta_3 S_v I_h - (\alpha_v + \delta_v) I_v; \\ {}_0^C D_t^\eta P &= P_1(t, P) = \delta_v (S_v + I_v) - \gamma_1 P. \end{aligned}$$

By implying the power law kernel with the fractional integration, getting

$$S_h(t_{k+1}) = S_{h0} + \frac{1}{\Gamma(\eta)} \sum_{w=2}^k \int_{t_w}^{t_{w+1}} S_{h1}(t, S_h) \zeta^{1-\varpi} (t_{k+1} - \zeta)^{\eta-1} d\zeta,$$

Recall the Newton Polynomial:

$$\begin{aligned} \mathcal{A}(t, S_h) &\simeq \mathcal{A}(t_{k-2}, S_{h(k-2)}) + \frac{1}{\Delta t} \left\{ \mathcal{A}(t_{k-1}, S_{h(k-1)}) - \mathcal{A}(t_{k-2}, S_{h(k-2)}) \right\} (\zeta - t_{k-2}) \\ &+ \frac{1}{2\Delta t^2} \left\{ \mathcal{A}(t, S_{hk}) - 2\mathcal{A}(t_{k-1}, S_{h(k-1)}) - \mathcal{A}(t_{k-2}, S_{h(k-2)}) \right\} (\zeta - t_{k-2}) (\zeta - t_{k-1}). \end{aligned} \quad (7.1)$$

Replacing (7.1) into above equations:

$$\begin{aligned} 1S_{h(k+1)} &= S_{h0} + \frac{1}{\Gamma(\eta)} \sum_{w=2}^k S_{h1}[t_{w-2}, S_h^{w-2}] t_{w-2}^{1-\varpi} \int_{t_w}^{t_{w+1}} (t_{k+1} - \zeta)^{\eta-1} d\zeta + \frac{1}{\Gamma(\eta)} \sum_{w=2}^k \frac{1}{\Delta t} \left\{ t_{w-1}^{1-\varpi} S_{h1}(t_{w-1}, S_h^{w-1}) \right. \\ &- t_{w-2}^{1-\varpi} S_{h1}[t_{w-2}, S_h^{w-2}] \left. \right\} \times \int_{t_w}^{t_{w+1}} (\zeta - t_{w-2})(t_{k+1} - \zeta)^{\eta-1} d\zeta + \frac{1}{\Gamma(\eta)} \sum_{w=2}^k \frac{1}{2\Delta t^2} \left\{ t_w^{1-\varpi} S_{h1}[t_w, S_h^w] \right. \\ &- 2t_{w-1}^{1-\varpi} S_{h1}(t_{w-1}, S_h^{w-1}) + t_{w-2}^{1-\varpi} S_{h1}[t_{w-2}, S_h^{w-2}] \left. \right\} \int_{t_w}^{t_{w+1}} (\zeta - t_{w-2})(\zeta - t_{w-1})(t_{k+1} - \zeta)^{\eta-1} d\zeta. \end{aligned}$$



The integral in the equations above can be calculated as follows:

$$\int_{t_w}^{t_{w+1}} (t_{k+1} - \zeta)^{\eta-1} d\zeta = \frac{(\Delta t)^\eta}{\eta} [(k-w+1)^\eta - (k-w)^\eta].$$

$$\int_{t_w}^{t_{w+1}} (\zeta - t_{w-2})(t_{k+1} - \zeta)^{\eta-1} d\zeta = \frac{(\Delta t)^{\eta+1}}{\eta(\eta+1)} [(k-w+1)^\eta(k-w+3+2\eta) - (k-w)^\eta(k-w+3+3\eta)].$$

$$\int_{t_w}^{t_{w+1}} (\zeta - t_{w-2})(\zeta - t_{w-1})(t_{k+1} - \zeta)^{\eta-1} d\zeta = \frac{(\Delta t)^{\eta+2}}{\eta(\eta+1)(\eta+2)} \left[ (k-w+1)^\eta \{2(k-w)^2 + (3\eta+10)(k-w) + 2\eta^2 + 9\eta + 12\} - (k-w)^\eta \{2(k-w)^2 + (5\eta+10)(k-w) + 6\eta^2 + 18\eta + 12\} \right].$$

Hence, getting finally

$$S_{h(k+1)} = S_{h0} + \frac{(\Delta t)^\eta}{\Gamma(\eta+1)} \sum_{w=2}^k S_{h1}[t_{w-2}, S_h^{w-2}] t_{w-2}^{1-\varpi} \left\{ \frac{(\Delta t)^\eta}{\eta} [(k-w+1)^\eta - (k-w)^\eta] \right\}$$

$$+ \frac{(\Delta t)^\eta}{\Gamma(\eta+2)} \sum_{w=2}^k \left\{ t_{w-1}^{1-\varpi} S_{h1}(t_{w-1}, S_h^{w-1}) - t_{w-2}^{1-\varpi} S_{h1}[t_{w-2}, S_h^{w-2}] \right\} \times \left\{ \frac{(\Delta t)^{\eta+1}}{\eta(\eta+1)} [(k-w+1)^\eta(k-w + 3 + 2\eta)(k-w)^\eta(k-w+3+3\eta)] \right\}$$

$$\frac{(\Delta t)^\eta}{\Gamma(\eta+3)} \sum_{w=2}^k \left\{ t_w^{1-\varpi} S_{h1}[t_w, S_h^w] - 2t_{w-1}^{1-\varpi} S_{h1}(t_{w-1}, S_h^{w-1}) + 6t_{w-2}^{1-\varpi} S_{h1}[t_{w-2}, S_h^{w-2}] \right\} \times \frac{(\Delta t)^{\eta+2}}{\eta(\eta+1)(\eta+2)} \left[ (k-w+1)^\eta \{2(k-w)^2 + (3\eta+10)(k-w) + 2\eta^2 + 9\eta + 12\} - (k-w)^\eta \{2(k-w)^2 + (5\eta+10)(k-w) + 6\eta^2 + 18\eta + 12\} \right].$$

Similarly for remaining equations of (2.2), do like as above equations of  $S_h(t)$ . This is the complete numerical scheme for model (2.2) in sense of Caputo fractional derivative.

### 8. SIMULATION EXPLANTATION

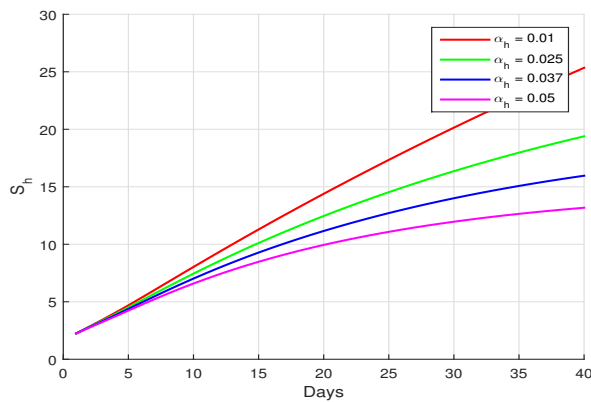


FIGURE 5. The impact of  $\alpha_h$  on healthy susceptible plants.

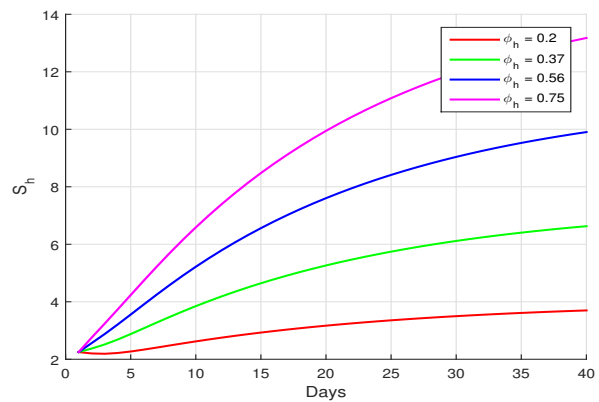


FIGURE 6. The impact of  $\phi_h$  on susceptible healthy plants.



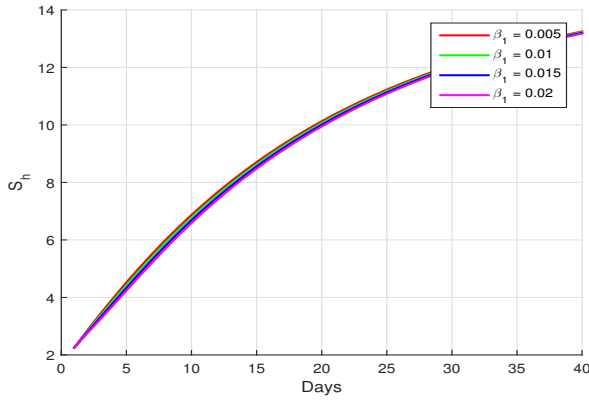


FIGURE 7. The impact of  $\beta_1$  on susceptible healthy plants.

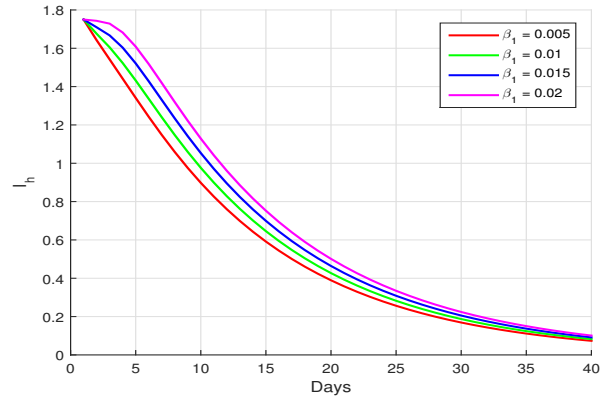


FIGURE 8. The impact of  $\beta_1$  on infected healthy plants.

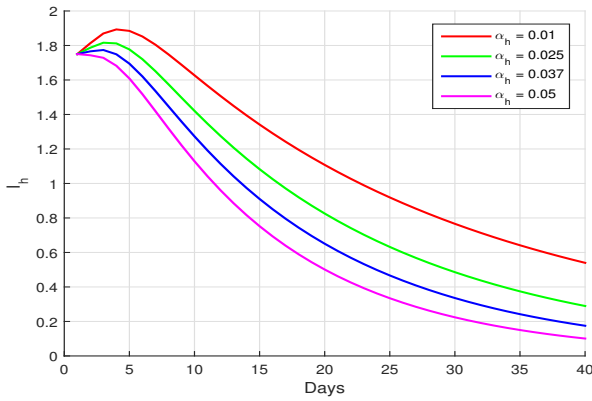


FIGURE 9. The impact of  $\alpha_h$  on infected healthy plants.

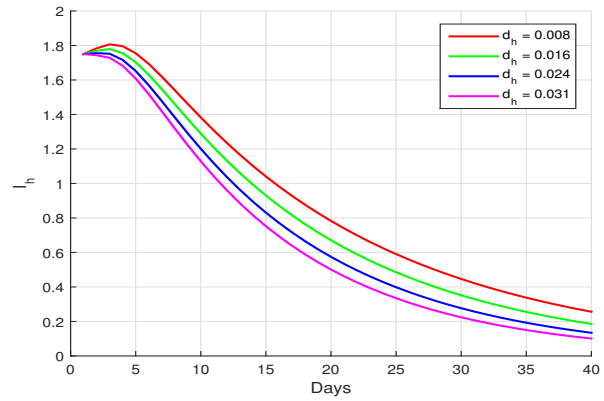


FIGURE 10. The impact of  $d_h$  on infected healthy plants.

**8.1. Simulation Explanation about Effect of parameters on Model.** The consequences of the model's primary and secondary parameters are depicted in the following images, with a focus on the infectious class to debate and examine the effects of various parameters. In order to determine whether the effects are directly or inversely proportional to the infectious class and whether the disease spreads to or emanates from the population, and also determine the range of the following factors.

Figure 5 see the relationship of  $\alpha_h$  and the susceptible healthy population, by the increasing of death rate  $\alpha_h$  also the susceptible healthy population is average decreasing. In Figure 6 see the relationship of  $\phi_h$  and the susceptible healthy population, by the increasing of birth rate  $\phi_h$  also the susceptible healthy population is sharply increasing. Figure 7 see the relationship of  $\beta_1$  and the susceptible healthy population, by the increasing of infectious disease rate of transformation  $\beta_1$  also the susceptible healthy population is increasing. Figure 8 see the relationship of  $\beta_1$  and the infected healthy population, by the increasing of infectious disease rate of transformation  $\beta_1$  also the infected healthy population is decreasing. Figure 9 see the relationship of  $\alpha_h$  and the infected healthy population, by the increasing of death rate  $\alpha_h$  also the infected healthy population is sloppy decreasing. Figure 10 see the relationship of  $d_h$  and the infected healthy population, by the increasing of infectious death rate  $d_h$  also the infected healthy population is sloppy



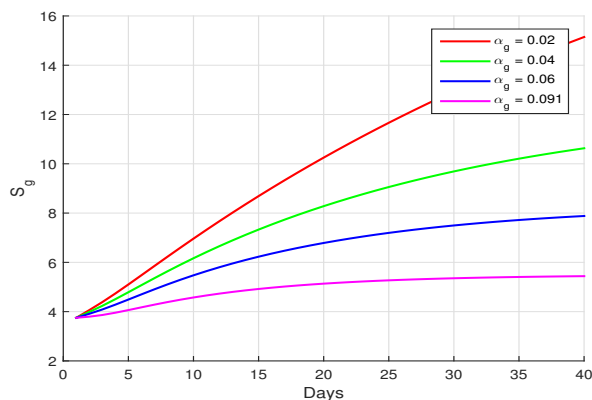


FIGURE 11. The impact of  $\alpha_g$  on susceptible growing plants.

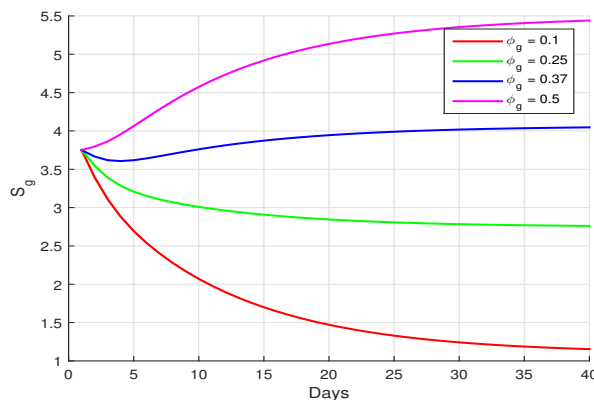


FIGURE 12. The impact of  $\phi_g$  on susceptible growing plants.

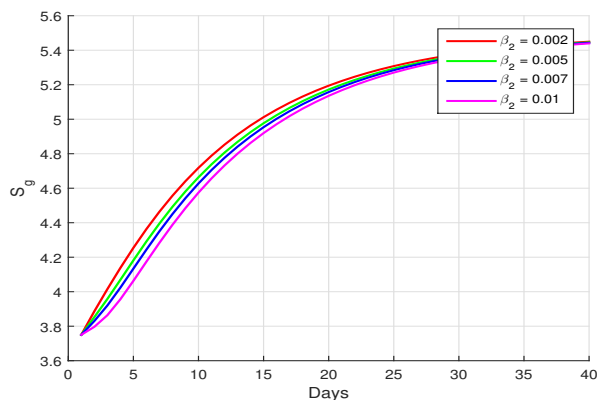


FIGURE 13. The impact of  $\beta_2$  on susceptible growing plants.

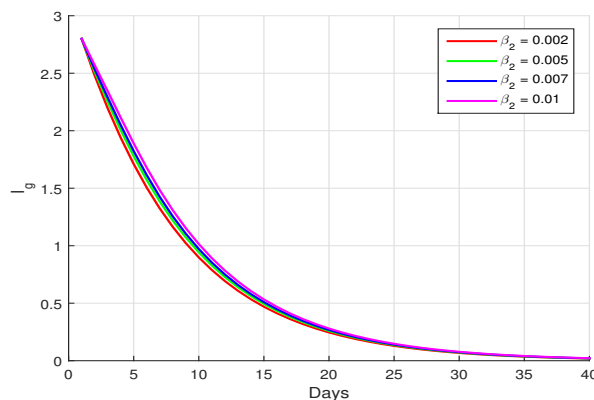


FIGURE 14. The impact of  $\beta_2$  on infected growing plants.

decreasing. Figure 11 see the relationship of  $\alpha_g$  and the susceptible growing population, by the increasing of natural death rate  $\alpha_h$  also the susceptible growing population is sharply decreasing. In Figure 12 see the relationship of  $\phi_g$  and the susceptible growing population, by the increasing of birth rate  $\phi_g$  also the susceptible growing population is sharply increasing. Figure 13 see the relationship of  $\beta_2$  and the susceptible growing population, by the increasing of infectious disease rate of transformation  $\beta_2$  also the susceptible growing population is increasing. Figure 14 see the relationship of  $\beta_2$  and the infected growing population, by the increasing of infectious disease rate of transformation  $\beta_2$  also the infected growing population is decreasing. Figure 15 see the relationship of  $\alpha_g$  and the infected growing population, by the increasing of natural death rate  $\alpha_g$  also the infected growing population is slopply decreasing. Figure 16 see the relationship of  $d_g$  and the infected growing population, by the increasing of infectious death rate  $d_h$  also the infected growing population is slopply decreasing. Figure 17 see the relationship of  $\alpha_v$  and the susceptible bacterial population, by the increasing of natural death rate  $\alpha_v$  also the susceptible bacterial population is decreasing. In Figure 18 see the relationship of  $\phi_v$  and the susceptible bacterial population, by the increasing of birth rate  $\phi_v$  also the susceptible bacterial population is increasing. Figure 19 see the relationship of  $\beta_3$  and the susceptible bacterial population, by the increasing of infectious disease rate of transformation  $\beta_3$  also the susceptible bacterial population is increasing. Figure 20 see the relationship of  $\beta_3$  and the infected bacterial population, by the increasing of infectious



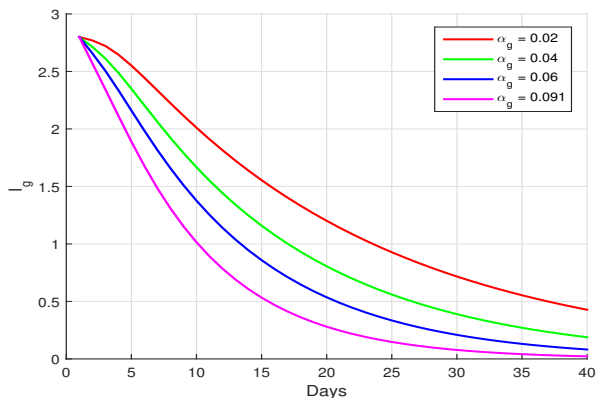


FIGURE 15. The impact of  $\alpha_g$  on infected growing plants.

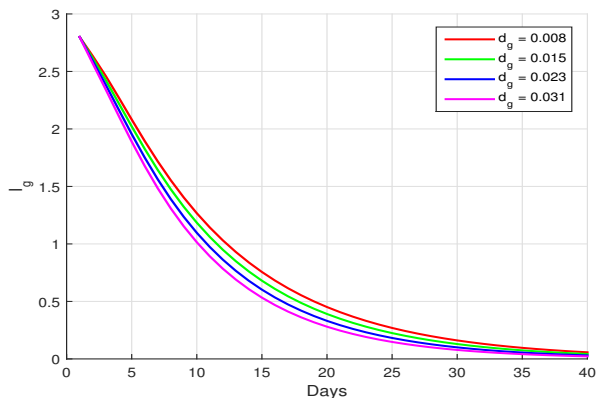


FIGURE 16. The impact of  $d_g$  on infected growing plants.

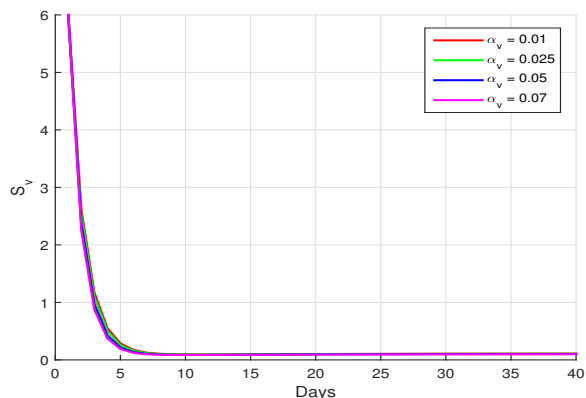


FIGURE 17. The impact of  $\alpha_v$  on susceptible vectors.

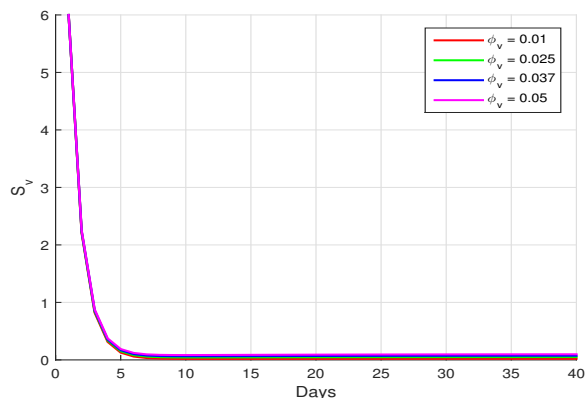


FIGURE 18. The impact of  $\phi_v$  on susceptible vectors.

disease rate of transformation  $\beta_3$  also the infected bacterial population is decreasing. Figure 21 see the relationship of  $\alpha_v$  and the infected bacterial population, by the increasing of natural death rate  $\alpha_v$  also the infected bacterial population is decreasing. Figure 22 see the relationship of  $\delta_v$  and the infected bacterial population, by the increasing of transmission rate  $\delta_v$  also the infected bacterial population is slopply decreasing. Figure 23 see the relationship of  $\delta_v$  and the susceptible bacterial population, by the increasing of transmission rate  $\delta_v$  also the susceptible bacterial population is decreasing. Figure 24 see the relationship of  $\delta_v$  and the pythagoreans population, by the increasing of transmission rate  $\delta_v$  also the pythagoreans is sharply increasing. Figure 25 see the relationship of  $\gamma_1$  and the pythagoreans population, by the increasing of decay rate  $\gamma_1$  also the pythagoreans is sharply decreasing. Figure 26 see the relationship of  $\phi_v$  and the pythagoreans population, by the increasing of birth rate  $\phi_v$  also the pythagoreans is sharply increasing.

**8.2. Simulation Explanation about Caputo Fractional Operator on Model.** The effectiveness of the derived theoretical consequences is illustrated by the following cases. The presentation of a mathematical analysis of rice taungro illness yields persuasive results when non-integer parametric parameters are used. By reducing the fractional values, the answer for  $S_h$ ,  $I_h$ ,  $S_g$ ,  $I_g$ ,  $S_v$ ,  $I_v$  and  $P$ , in Figure 16–22 approaches the desired value. The numerical



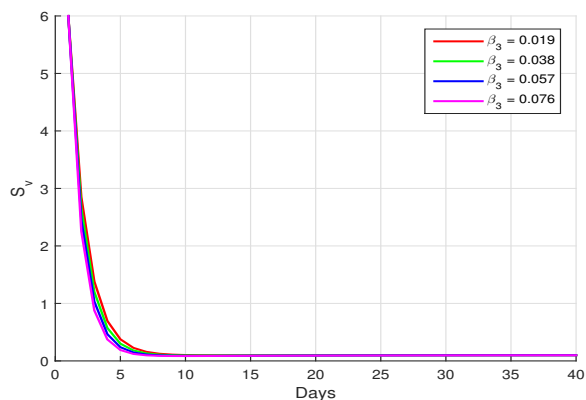


FIGURE 19. The impact of  $\beta_3$  on susceptible vectors.

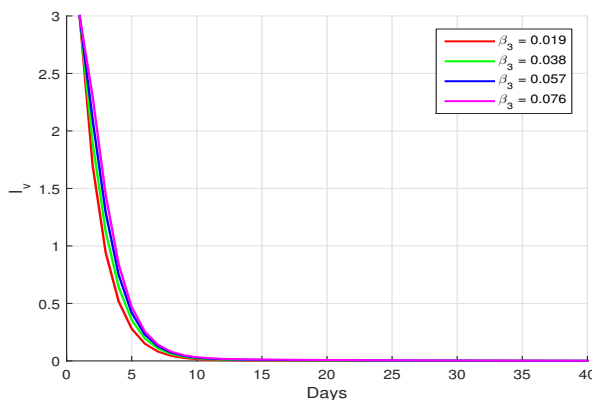


FIGURE 20. The impact of  $\beta_3$  on infected vector.

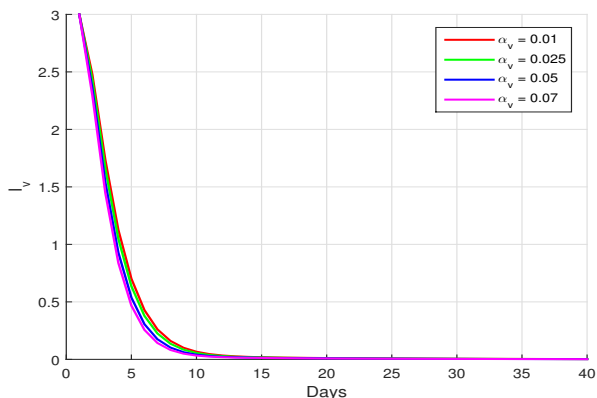


FIGURE 21. The impact of  $\alpha_v$  on susceptible vectors.

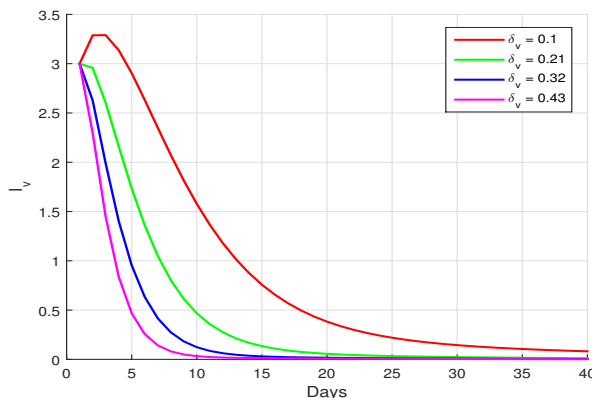


FIGURE 22. The impact of  $\delta_v$  on infected vectors.

simulation for the fractional order rice taungro disease model is found using MATLAB code. The system's initial values are  $S_h(0) = 2.25$ ,  $I_h(0) = 1.75$ ,  $S_g(0) = 3.75$ ,  $I_g(0) = 2.80$ ,  $S_v(0) = 6$ ,  $I_v(0) = 3$  and  $P(0) = 5.5$  for each of the sub-compartments. The system's parametric values are  $\phi_h = 0.75$ ,  $\beta_1 = 0.02$ ,  $\alpha_h = 0.05$ ,  $d_h = 0.031$ ,  $\phi_g = 0.5$ ,  $\beta_2 = 0.01$ ,  $\alpha_g = 0.091$ ,  $d_g = 0.031$ ,  $\phi_v = 0.05$ ,  $\beta_3 = 0.076$ ,  $\alpha_v = 0.057$ ,  $\delta_v = 0.43$  and  $\gamma_1 = 0.021$ . Show the graphical representation of the rice taungro disease model using the suggested numerical method in Figures 27–33, and compare the integer order result with the fractional order result. The dynamics of healthy plants susceptible  $S_h$  and growing plants susceptible  $S_g$  rice taungro caused by disease are shown in Figures 27 and 29, respectively. In these scenarios, all of the compartments had a sloped upward inclination, and after some time, they approached a steady position because to a rise in recovered. The dynamics of plants healthy infected  $I_h$ , plants growing infected  $I_g$ , susceptible vector  $S_v$  and infected vector  $I_v$  are shown in Figures 28, 30, 31, and 32, respectively. In these scenarios, all of the compartments rigidly sloped downward, as the recovered situation increased, the compartments approached a stable state. Furthermore, pythagoreans with and without medication grow by lowering the fractional values, as seen in Figure 33. It forecasts the future directions of this research and how can reduce the number of diseased plants and infected vectors that proliferate in the environment. For all sub-compartments at fractional derivatives, the Caputo



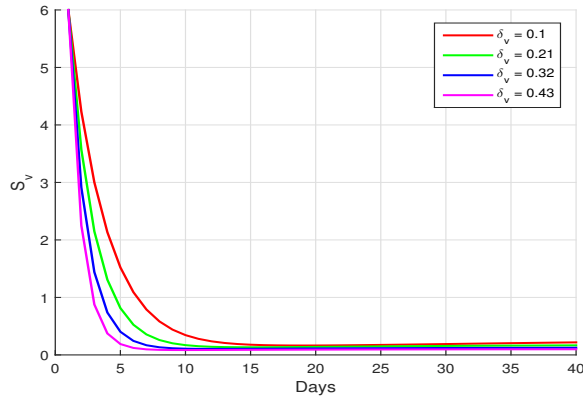


FIGURE 23. The impact of  $\delta_v$  on susceptible vectors.

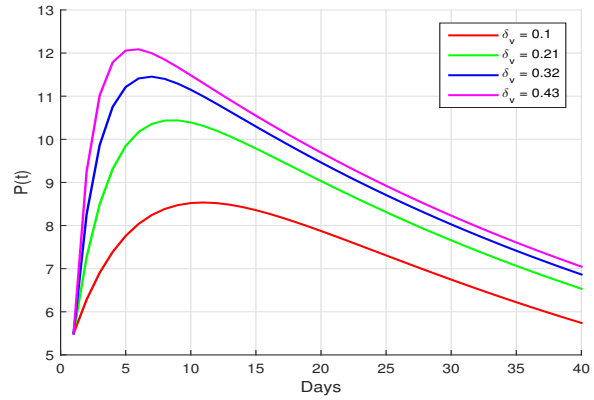


FIGURE 24. The impact of  $\delta_v$  on pythagoreans.

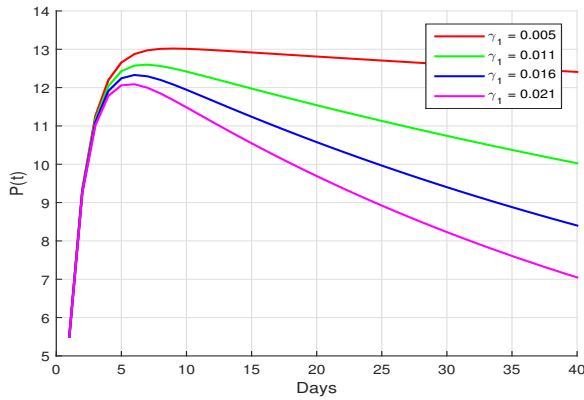


FIGURE 25. The impact of  $\gamma_1$  on pythagoreans.

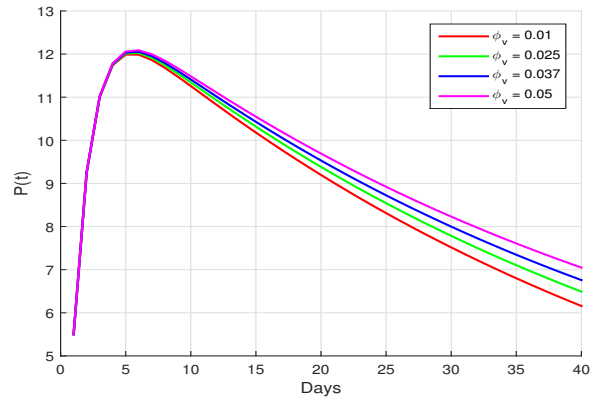


FIGURE 26. The impact of  $\phi_v$  on pythagoreans.

fractional operator produces superior results compared to standard derivatives. Additionally, it is proposed that the solutions for all compartments become more precise and dependable when fractional values are decreased.

### 9. CONCLUSION

A nonlinear compartmental model has been proposed as a possible explanation for the transmission of rice taungro disease for plants. In order to validate the real locations of equilibria in the proposed model, a qualitative study has been carried out in addition to a quantitative analysis. Reproductive number, which illustrates how quickly rice taungro spreads throughout its various compartments and is an essential indicator of the likelihood that an epidemic may occur in the environment. The nonlinear ordinary differential equations of the model were thoroughly examined for well-posedness. The nonlinear functional analysis is used to ascertain the presence and positive solution with the help Banach space results. Using the Lyapunov function, it is also demonstrated that the suggested rice taungro disease is globally asymptotically stable under created hypothesis. There is widespread consensus on system management; the rice taungro disease investigated with a fractional derivative for continuous monitoring, controls the essential lowest transfer rate. The graph illustrates the time-varying effects of several variables on the quantity of the crucial spread of disease as a plant virus. The effects of the fractional operator are explored by generating Lagrange polynomial solutions



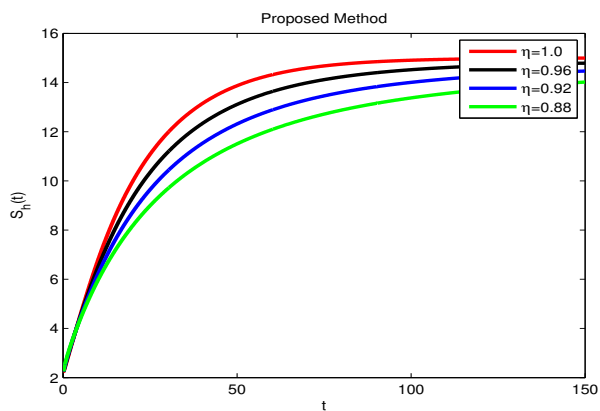


FIGURE 27. Segment Simulation under Caputo for  $S_h(t)$ .

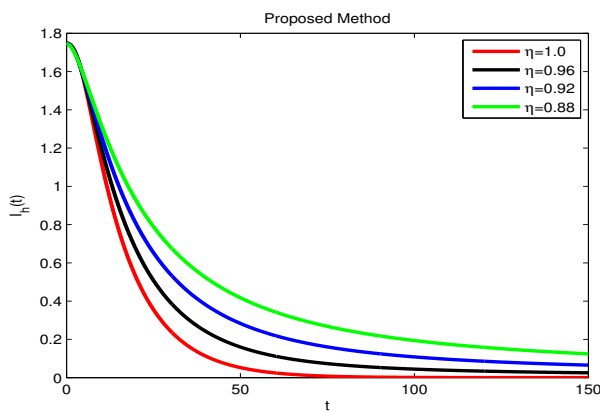


FIGURE 28. Segment Simulation under Caputo for  $I_h(t)$ .

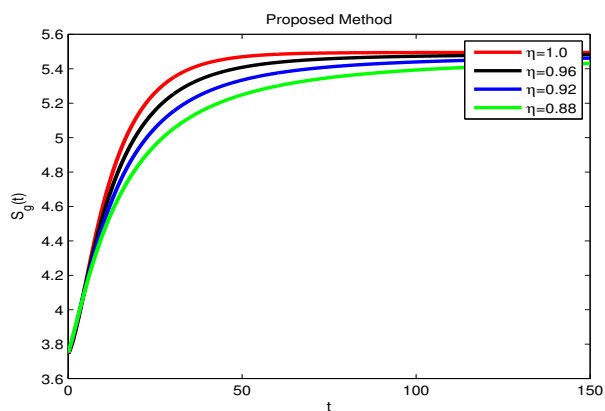


FIGURE 29. Segment Simulation under Caputo for  $S_g(t)$ .

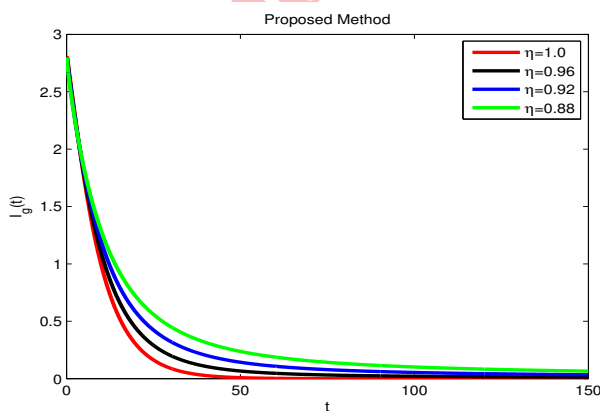


FIGURE 30. Segment Simulation under Caputo for  $I_g(t)$ .

in two steps through numerical simulations. This shows how the many contributing factors to rice taungro have an impact on the environment under consideration. In order to record complex and nonlocal interactions, the rice taungro disease model employs for observing the accurate description of the behavior in simulation under different fractional values which shows hypersensitive response (HR) to provide resistances against bacterial splashing-rain. This method advances understanding of the disease by improving long-term behavior forecasts and illuminating its intricacies by treatment as well as early detection of different infected plants on the regular basis for healthy environment. This kind of analysis helps to manage and understand the spread as well as control of rice taungro infections within the environment, also helpful for future control and research strategies to lessen the disease's effects.

FUNDING

No funding.

DATA AVAILABILITY

No data.



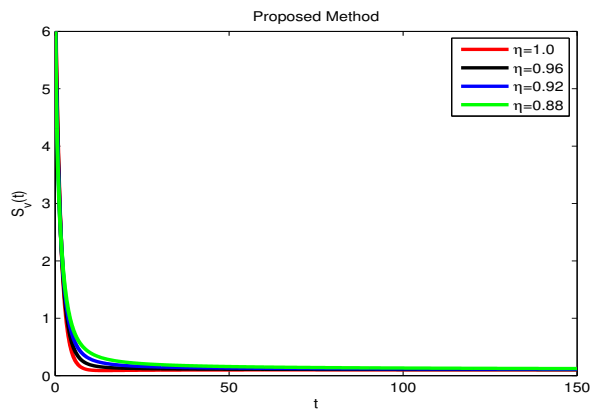


FIGURE 31. Segment Simulation under Caputo for  $S_v(t)$ .

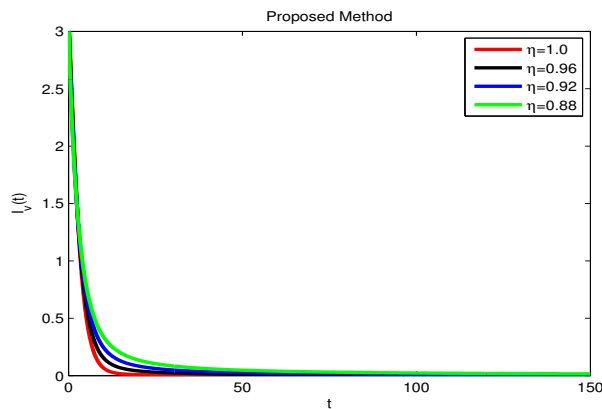


FIGURE 32. Segment Simulation under Caputo for  $I_v(t)$ .

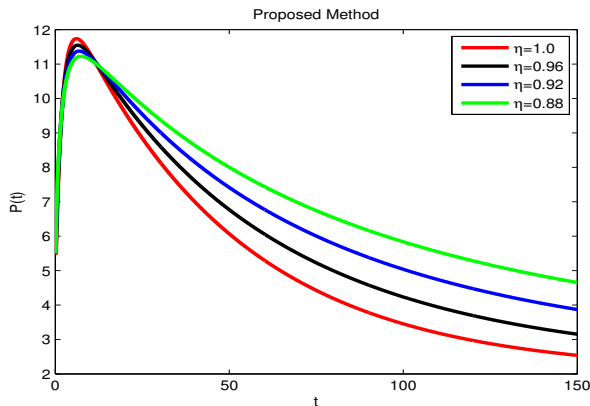


FIGURE 33. Segment Simulation under Caputo for  $P(t)$ .

REFERENCES

- [1] M. E. Abo and H. A. Fadhilab, *Epidemiology and management of rice viruses and virus diseases*, Plant Virology in Sub-Saharan Africa: Proceedings of a Conference Organized by IITA: 4–8 June 2001, International Institute of Tropical Agriculture, Ibadan, Nigeria, IITA, (2003), p. 112.
- [2] A. Ahmad, F. Abbas, M. Farman, E. Hincal, A. Ghaffar, A. Akgül, and M. K. Hassani, *Flip bifurcation analysis and mathematical modeling of cholera disease by taking control measures*, Scientific Reports, 14(1) (2024), 10927.
- [3] A. Ahmad, K. Faiz, A. Ghaffar, G. Mustafa, and E. Hincal, *Bifurcation and control of Xanthomonas infectious disease spread in banana plants under hypersensitive response*, Aerobiologia, 2025, 1–27.
- [4] A. Ahmad, K. Faiz, M. Farman, S. Sattar, and A. Sambas, *Control and effect of climate change due to human activities by mathematical modeling approach under fractional operator*, Modeling Earth Systems and Environment, 11(4) (2025), 1–21.
- [5] A. Ahmad, M. Farman, A. Akgül, K. S. Nissar, and A. H. A. Aty, *Mathematical analysis of fractional order diarrhea model*, Progr. Fract. Differ. Appl, 9(1) (2023), 41–58.



- [6] A. Ahmad, M. Farman, A. Akgül, K. S. Nissar, and A. H. A. Aty, *Mathematical analysis of fractional order diarrhea model*, *Progr. Fract. Differ. Appl.*, 9(1) (2023), 41–58.
- [7] A. Ahmad, M. Farman, P. A. Naik, and A. Akgul, *Modeling of smoking transmission dynamics using Caputo–Fabrizio type fractional derivative*, *Computational and Analytic Methods in Biological Sciences*, River Publishers, (2023), 1–20.
- [8] A. Ahmad, M. Farman, P. A. Naik, K. Faiz, A. Ghaffar, E. Hincal, and M. U. Saleem, *Analytical analysis and bifurcation of pine wilt dynamical transmission with host vector and nonlinear incidence using sustainable fractional approach*, *Partial Differential Equations in Applied Mathematics*, 11 (2024), 100830.
- [9] A. Ahmad, Q. M. Farooq, H. Ahmad, D. U. Ozsahin, F. Tchier, A. Ghaffar, and G. Mustafa, *Study on symptomatic and asymptomatic transmissions of COVID-19 including flip bifurcation*, *International Journal of Biomathematics*, 17(2) (2024), 2450002.
- [10] A. Ghaffar, K. Faiz, A. Ahmad, G. Mustafa, and M. Farman, *Bifurcation and control of rice tungro disease spread in plants under hypersensitive response*, *Punjab University Journal of Mathematics*, 56(11) (2024), 723–752.
- [11] A. Ghaffar, K. Faiz, and A. Ahmad, *Investigation and bifurcation analysis of the ocean system impact on climate change utilizing mathematical modeling approach*, *Modeling Earth Systems and Environment*, 11(3) (2025), 1–22.
- [12] N. J. Cunniffe, B. Koskella, C. J. E. Metcalf, S. Parnell, T. R. Gottwald, and C. A. Gilligan, *Thirteen challenges in modelling plant diseases*, *Epidemics*, 10 (2015), 6–10.
- [13] F. Dayan, N. Ahmed, A. H. Ali, M. Rafiq, and A. Raza, *Numerical investigation of a typhoid disease model in fuzzy environment*, *Scientific Reports*, 13(1) (2023), 21993.
- [14] A. Devaux, J. P. Goffart, A. Petsakos, P. Kromann, M. Gatto, J. Okello, V. Suarez, and G. Hareau, *Global food security, contributions from sustainable potato agri-food systems*, *The Potato Crop: Its Agricultural, Nutritional and Social Contribution to Humankind*, (2020), 3–35.
- [15] M. Farman, A. Ahmad, A. Zehra, K. S. Nisar, E. Hincal, and A. Akgul, *Analysis and controllability of diabetes model for experimental data by using fractional operator*, *Mathematics and Computers in Simulation*, 218 (2024), 133–148.
- [16] M. Farman, Q. B. Rasheed, M. U. Saleem, and A. Ahmad, *Modelling and analysis of the fractional order Ebola virus model with Caputo–Fabrizio derivative*, *Punjab University Journal of Mathematics*, 52(10) (2020).
- [17] M. Farman, M. U. Saleem, A. Ahmad, S. Imtiaz, M. F. Tabassum, S. Akram, and M. O. Ahmad, *A control of glucose level in insulin therapies for the development of artificial pancreas by Atangana–Baleanu derivative*, *Alexandria Engineering Journal*, 59(4) (2020), 2639–2648.
- [18] D. D. Headey, *The impact of the global food crisis on self-assessed food security*, *The World Bank Economic Review*, 27(1) (2013), 1–27.
- [19] U. IFAD, *The state of food security and nutrition in the world 2017*, FAO, (2017).
- [20] B. Jin and B. Jin, *Cauchy problem for fractional ODEs*, *Fractional Differential Equations: An Approach via Fractional Derivatives*, (2021), 97–136.
- [21] J. W. Jones, J. M. Antle, B. Basso, K. J. Boote, R. T. Conant, I. Foster, H. C. J. Godfray, M. Herrero, R. E. Howitt, and S. Janssen, *Brief history of agricultural systems modeling*, *Agricultural Systems*, 155 (2017), 240–254.
- [22] M. O. Kulachi, A. Ahmad, E. Hincal, A. H. Ali, M. Farman, and M. Taimoor, *Control of conjunctivitis virus with and without treatment measures: a bifurcation analysis*, *Journal of King Saud University–Science*, 36(7) (2024), 103273.
- [23] P. S. Rao and A. Hasanuddin, *Incidence of rice tungro virus disease and its vector in South Sulawesi, Indonesia*, *International Journal of Pest Management*, 37(3) (1991), 256–258.
- [24] F. Wang, M. N. Khan, I. Ahmad, H. Ahmad, H. A. Zinadah, and Y. M. Chu, *Numerical solution of traveling waves in chemical kinetics: time-fractional Fisher’s equations*, *Fractals*, 30(2) (2022), 2240051.

